The Physics of Sand Dune Formation and Migration on Mars

A Major Qualifying Project Report

Submitted to the Faculty

of the

WORCESTER POLYTECHNIC INSTITUTE

in partial fulfillment of the requirements for the

Degree of Bachelor of Science

in Physics

by

Michael J. Kavulich Jr.

Date: April 27, 2008

Abstract

Sand dunes have been observed throughout the surface of the planet Mars. Movement of these dunes has been theorized and inferred from the lack of craters on dunes. Dune movement has not yet been directly imaged, however. Understanding sand movement processes is vital to a correct Martian climate model, as well as the safety of future missions to Mars.

Imagery from several Martian orbiters was analyzed in an attempt to discern movement of Martian sand dunes. Additional imagery from Mars Exploration Rover Opportunity was analyzed to search for evidence of dune movement or saltation at Meridiani Planum, Mars. Data from Opportunity shows that a saltation event occurred sometime in July 2007, at the rim of Victoria Crater. No dune movement was detected, suggesting that dune movement, if it occurs on Mars, is on the scale of centimeters or less per Martian year. Future studies should benefit from added high-resolution satellite imagery, which is currently being collected by the Mars Reconnaissance Orbiter, and, if current theories on dune movement are correct, dune movement should be discernable within a few years.

1. Introduction

On Earth, sand is a very plentiful resource. Wind, water and ice, as well as chemical reactions and biological activity, all serve to break apart rocks and other solid material into sand on a large scale. While much of this sand is quickly stabilized by biological and hydrological processes, and converted into sedimentary rock, some of it, especially in desert climates where these influences are minimal, remains in the form of unconsolidated sand and dust for thousands of years or more, subject to influence by the wind.

Sand is an especially interesting material to study because of its granular nature. When acted upon by wind, sand behaves in ways that, at first glance, seem peculiar. Instead of being deposited evenly along a surface, sand self-accumulates into ripples, drifts, and dunes. It can be piled high, but can only sustain slopes up to the material's angle of repose for the local gravitational force, beyond which the pile will undergo gravitational collapse.

Sand dunes cover an estimated 5,000,000 km^2 of Earth's surface (more than half the area of the United States), mostly in desert climes and along shorelines (Hayward et al., 2007). Where surface sand dominates, it can present a serious hazard to machinery when made airborne. For example, sand storms famously foiled President Jimmy Carter's attempt to rescue American hostages being held in Iran in 1980. Granules of sand and dust are so small that they can sneak through microscopic gaps into the workings of complex machinery, causing serious malfunctions and short-circuits. The abrasive action of airborne sand can damage or destroy structures and equipment alike. Unchecked, dunes can cover and rend useless vitually anything downwind: roads, machinery, even entire settlements (Hayward et al., 2007; Jones, 2001).

It has been apparent that dunes exist on Mars since 1971, when Mariner 9 imaged the first extraterrestrial dune fields (Iverson, 1976). Observations of extensive dune fields across the Red Planet in 1972, as well as the absence of any substantial liquid water or geological activity on the present Martian surface, make it clear that aeolian processes are indeed the dominant geomorphic forces which are shaping present-day Mars (Phillips, 1998).

The United States' "Vision for Space Exploration" includes stipulations for future exploration of Mars by both unmanned probes and crewed missions (Bush, 2004). With a clear goal of establishing the presence of complicated machinery, where great expenditures and potentially the lives of astronauts will be at stake, it is absolutely essential to understand the mechanics of aeolian processes as they take place on Mars. An essential part of this understanding would be determining the activity of the current Martian surface.

Despite several successful lander and rover missions to Mars in the past few decades, as well as a steady improvement in the resolution of images taken from orbit, there is still no hard evidence of dune movement *anywhere* on present-day Mars (Williams, 2006). This study sought to use available imagery from Mars orbiters and *Opportunity* rover to search for any dune movement. The analysis concluded that saltation is likely occurring during the most severe storms on present day Mars, and that one saltation event likely occurred as recent as July, 2007. However, no conclusive evidence for dune movement on present-day Mars was found.

2. Background

2.1 The nature of sand on Earth

Sand covers 20% of Earth's deserts (Watson, 1997), while deserts cover approximately 20% of Earth's surface. It is created by the erosion of rock containing quartz, feldspar, or other hard minerals, as well as the erosion of coral and volcanic glass. Sand is mainly found near seashores, where it is created by wave action, along rivers, where rocks frequently collide in strong currents, and in deserts, where it is created by aeolian processes.

It seems natural, when dealing with a problem of sand movement, to first define exactly what sand is. Sand is a subset of all granular materials. Granular materials can be as large as boulders, and can be as small as 1 μm (the scale where thermal vibration effects become significant). Sand can be defined as any granular material which can be influenced by fluid flow, however, this definition must be restricted one degree further by putting a limit on the diameter of the material's individual grains. The need for this restriction is clear; while both a fine powder and a heap of boulders fit neatly into the granular material definition, they behave quite unlike traditional sand under a fluid in motion. A powder will be dispersed quite quickly and suspended, while larger rocks will be entirely unaffected, disregarding abrasive erosion.

The definition of sand used by Bagnold is a very good general one for the purpose of dune study (Bagnold, 1941). A lower limit for sand grain size can be found by investigating the behavior of a fluid flowing over a granular surface. In natural situations, fluid flow is very rarely fully laminar; it will contain eddies, or "gusts", which represent a local increase in wind speed and change in direction. Some of these eddies will be in an upward direction, giving the potential for small particles to be suspended. However, nearer to the ground, the upward and downward components of the eddies are weaker than other directions. While the intensity of these upward gusts is variable, it is commonly approximated as 20% of the mean wind velocity

(Alghamdi and Akyurt, 2001). Therefore, any particle with a terminal velocity lower than 0.2 times the mean wind velocity will be carried up and suspended indefinitely, provided the wind keeps up. Any particle which can achieve this suspension is defined as *dust*.

An upper limit for sand grain size is even easier to define. Sand moves through two modes of transport: *saltation* and *surface creep*. There is an additional mode, *reptation*, which is the minor saltation of sand grains physically dislodged by impacting particles, which typically do not have the energy to dislodge further grains (Lancaster, 1995; Parteli, 2007). However, as is apparent by the definition, reptation is merely a subset of saltation, and so shall be included within this category.

Saltation is the process where by sand grains actually become airborne, while surface creep is sand movement by which the grains never actually leave the ground. At some upper limit, however, the combination of wind pressure and sand impact are no longer sufficient to move a grain of sufficient size. Grains which remain stationary even in the most intense wind are defined as *pebbles*. Therefore, any granular material which does not fall under the definition of dust or pebbles is *sand*.

Natural sand never consists of uniformly-sized grains. There will always be some natural variation in the size of sand grains, even those formed from the same rock and by the same process. The distribution of sand grain sizes is known as the *grading* of the sand.

2.2 Nature of sand movement

Fluid-based sand transport takes place close to the planetary surface, within what is known as the *boundary layer*; the layer of wind above the ground where surface friction affects the local wind velocity. Within the boundary layer, wind tends to vary logarithmically by height, defined by Equation 1.

$$u(z) = \frac{u_*}{\kappa} \ln \frac{z}{z_0} \qquad (1)$$

The terms used in this equation will be defined later, however there is an important term to point out now: u_*, which is known as the *shear velocity*. The shear velocity is not an actual velocity, but a mathematical parameter of a wind profile with *units* of velocity. The shear velocity is constant for a given wind profile, so it is considered more convenient, in discussions of sand movement and other near-surface processes, to refer to boundary layer winds in terms of shear velocity rather than actual velocity.

A single grain can be moved in a variety of ways. It can be moved as part of a sand avalanche on a slip face or it can be knocked forward along the ground (or even into the air) by an impacting airborne grain. When analyzing the initiation of sand movement, however, it is necessary to study the case where a sand grain is moved by the direct pressure of the wind.

A sand sheet is obviously stable under a fluid with no velocity. At very low velocities, friction between individual grains in the sand sheet keeps them from moving. However, as wind velocity increases, eventually drag and lift forces overcome the forces of friction and gravity keeping the sand grains in place, and the most exposed sand grains will become airborne (Lancaster, 1995).

A grain lifted in this manner will likely have a small initial velocity in relation to the mean wind velocity at its initial height. Therefore, the faster wind will impart some of its momentum upon this grain, possibly reaching an equilibrium, where the grain is moving at the local wind speed. However, the airborne state of the sand particle is short-lived. When the particle impacts the sand bed, it transfers its momentum, usually into several sand grains. In this way, even grains not exposed enough or too large to be moved by the fluid threshold shear velocity may be dislodged and set in motion, which initiates a type of sand movement known as *saltation*. Saltation is a mode of sand movement involving short jumps by individual particles, and is the process by which approximately 75% of sand movement occurs (Bagnold, 1941).

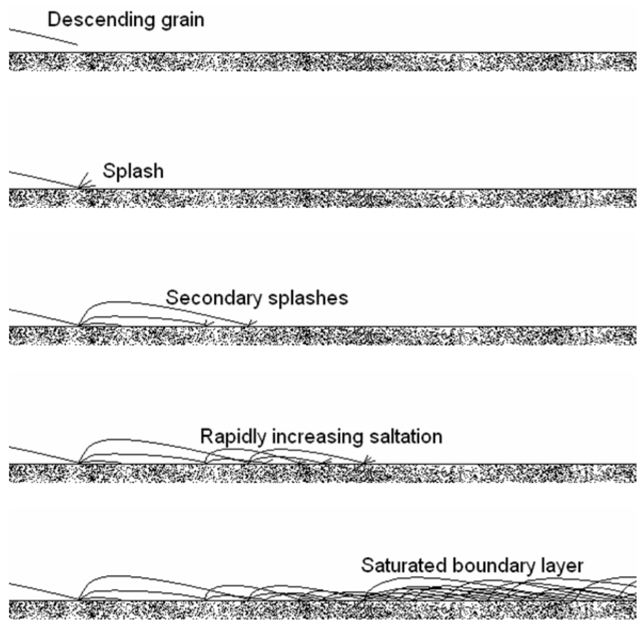

Figure 1: Initiation of saltation. A single grain dislodged by the wind can create a cascade of saltating grains. In this way, a wind which blows for even a short while can move a significant amount of sand.

When the grain impacts the sand bed, it creates a *splash*, which is the propulsion of multiple sand grains at the impact site into the wind stream. If the wind remains constant at or above u_{*ft}, the flux of saltating grains q will initially increase exponentially as more and more grains are impacted and driven into the wind stream. Since each additional saltating grain draws more momentum from the wind, the wind speed in the saltation layer decreases. Eventually, the system reaches an equilibrium airborne grain density, where the force of the wind lifts as many grains as it possibly can into saltation.

In addition to increasing the number of grains in saltation, impacting grains also serve to initiate another type of sand movement, known as *surface creep*. Even though grains that are a bit too large to saltate by direct wind pressure can be dislodged by impacting grains, other grains are too large to become airborne even when given this extra boost of momentum. However, if these grains are not too large, they may be knocked forward along the sand surface without ever becoming airborne. This is the process of surface creep: descending grains impact other larger grains, moving them forward slightly before friction stops them.

Once saltation has been initiated, the main producer of saltating particles is the impact of other saltating particles on the sand bed. A peculiar consequence of this property is that after the initiation of saltation, the shear velocity may drop below u_{*ft}, and saltation will still continue. At this point, the fluid threshold shear velocity becomes unimportant, and a new, lower threshold comes to light. It is only when the shear velocity drops below this new level, the *impact threshold shear velocity* (u_{*t}), that saltation will cease.

The aforementioned saturation of the boundary layer is not an instantaneous process. For any given grain distribution and wind speed, there is a lag between the time saltation is initiated and when the maximum grain density is reached. The *saturation length* is the distance a parcel of fluid moves before achieving the maximum grain density (Bagnold, 1941). It also represents a rough measure of the distance it takes for a change in one property of the wind flow to reform into a new velocity profile according to Equation 1.

Sand movement, taken on the level of individual grains, is understandably chaotic. A single wind-blown grain impacting the surface can knock multiple grains into random trajectories. However, taking the average paths of individual saltating grains gives the *characteristic path* for a given sand and wind. The length of this path is the *saltation length*, L_s, an important parameter in many sand transport models, as well as in the formation of ripples, which will be described later (Bagnold, 1941).

The velocity distribution of the wind in the boundary layer is roughly logarithmic by height, as can be seen in Equation 1. However, the level at which the velocity actually drops to zero is slightly above the actual ground level. In fact, for different values of shear velocity over the same surface, the wind speed drops to zero at the same height. This term, z_0, is known as the *surface roughness*, which will be explained later. It changes greatly between different types of terrain, and is dependant mainly on the degree of sand movement and dominant grain size.

3. Physics of sand movement

Sand, a granular material, has some properties of a fluid, some properties of a solid, and some of neither. As such, it requires unique equations to describe its behavior, particularly when under the influence of a flowing fluid.

Some of the first equations to accurately predict the movement of sand and sand formations were formulated by Ralph A. Bagnold. His book, *Physics of Blown Sand and Desert Dunes*, was the first comprehensive study on all forms of sand transport. It is still used actively many decades later, and may still be the best work on the physics of sand dunes. Many of his original equations will be useful in this analysis.

Within the planetary boundary layer, mean wind velocity u varies logarithmically with height z according to the relation shown here

$$u(z) = \frac{u_*}{\kappa} \ln \frac{z}{z_0} \qquad (1)$$

where $\kappa = 0.40$ is the von Kármán constant (AMS, 2000), u_* is the wind shear velocity, and z_0 is the *surface roughness*. The terms u_* and z_0 are independent variables which may be determined experimentally. The von Kármán constant does not depend on atmospheric properties; it is an experimentally derived universal constant. It should be noted that z_0 is not an actual measure of *surface roughness*, but an apparent measure, which will be explained later.

With the wind velocity distribution known, it is natural to investigate what strength of wind is needed to initiate sand movement. Individual sand grains are rough, irregular chunks of material, varying widely from the theoretical spherical shape. Therefore, as Bagnold pointed out, it is convenient to find a scaling factor for determining the diameter of a sphere of equivalent composition as the non-spherical sand grains which will behave identically under the influence of a fluid. This *shape factor* is dependant largely upon the amount of weathering that the sand has undergone, as well as the average grading of the sand. It must often be determined experimentally; for desert sand on Earth, 0.75 is a good approximation. (Bagnold, 1941) Multiplying the actual average diameter of sand grains by the shape factor yields the apparent grain diameter, which will be used from here on in place of the actual grain diameter.

There are actually two forces imparted upon an exposed sand grain by the wind. (Parteli, 2007) The first, a *drag force*, is due to the friction of the moving air on the grain, and is in the direction of the fluid flow. It is described by the equation

$$F_d = \beta u_*^2 \frac{\sigma \pi d^2}{4} \qquad 2$$

where d is the diameter of the particle, σ is its density, β is a constant which depends on the packing of the grains, and u_* is the *shear velocity*. The second force, the *lift force*, is

$$F_l = \Delta p \frac{\sigma \pi d^2}{4} \qquad 3$$

where Δp is the difference in pressure from the bottom to the top of the grain. On the scale of sand grains, due to the strong velocity gradient near the surface, the lift force is very significant. On Earth, it is approximately equal to 85% of the magnitude of the drag force.

At the initiation of sand movement, the drag and lift forces work to rotate the grain over some pivot point *p*. These forces are resisted by the grain's weight, which is

$$F_g = g \cdot (\sigma - \rho)\frac{\pi d^3}{6} \qquad 4$$

where ρ is the density of the fluid and *g* is the planetary gravitational constant. Thus, with a momentum balance, it is easily possible to find the threshold parameters for grain movement.

The forces balance over a pivot point *p* seen on the right. Therefore, when (5) is true,

$$F_d \cos\phi \leq (F_g - F_l)\sin\phi \qquad 5$$

the saltation process begins (Parteli, 2007).

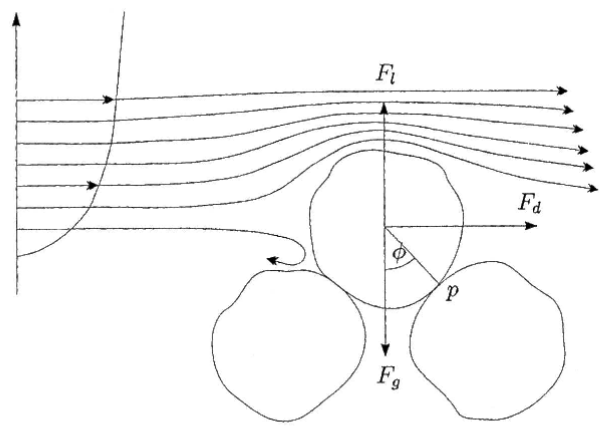

Figure 2: Forces governing the initiation of sand movement. From Parteli, 2007.

There are several important parameters which govern sand movement, as well as two important thresholds which indicate when movement will begin. Under unchanging topographic conditions, the shear velocity is defined by another important quantity, the *shear stress*, τ_f according to the relation

$$u_* = \sqrt{\frac{\tau_f}{\rho}} \qquad 6$$

where ρ is the density of the fluid. The shear stress is merely a measure of the drag force per unit surface area.

As the shear velocity increases, the drag force and lift force increase as well. The value of u_* where the inequality shown in (5) is true is called the *fluid threshold shear velocity* (u_{*ft}). An equation for u_{*ft} is

$$u_{*ft} = A\sqrt{\frac{\sigma - \rho}{\rho} gd} \qquad 7$$

where A is the *Shields parameter*. The Shields parameter has been determined experimentally in the past, and is relatively constant on Earth. Under low atmospheric pressure, however, the Shields parameter has a complex dependence upon the grain diameter and wind velocity.

At the fluid threshold, the most exposed sand grains begin to be entrained in the fluid. Because the velocity of the wind works parallel to the surface, the motion of the grain is temporary; soon, any upward motion of the grain is checked by the grain's weight, and the grain impacts the sand bed some distance downstream (Bagnold, 1941).

As mentioned above, the additional momentum imparted to grains on impact allows grains of larger sizes to enter saltation. Thus after the initiation of saltation the *impact threshold shear velocity* (u_{*t}) becomes the more important parameter. It is typically near 80% of the value of u_{*ft} (Parteli, 2007).

If dune movement is indeed occurring, then an important factor to know is the sand flux q, or the weight of sand transported per second. Here is where Bagnold's work becomes insufficient, as his sand flux equations are fairly accurate, but do not predict the existence of a threshold velocity. A universal sand flux equation, which has been confirmed by both wind tunnel and field experiments, here shown as Equation 8 (White, 1979; Lancaster, 1995).

$$q = 2.61 \cdot \frac{u_*^2 \rho}{g} \left(1 - \frac{u_{*t}}{u_*}\right)\left(1 + \frac{u_{*t}^2}{u_*^2}\right)$$

The problem, then, for determining the existence of dune movement on Mars through calculation, lies in the knowledge of several key features of the local Martian surface. Indeed, it is very possible that there are places on Mars where saltation still occurs, and others where aeolian features are "petrified", no longer influenced by the prevailing winds.

4. Dune formation and movement

4.1 Small-scale sandforms

Sand under the influence of wind can be found in many different formations, dependant upon many factors, including grain size, average shear velocity, sand availability, and the presence of obstacles. *Sandform* is a generic term for any sandy deposit or formation.

The simplest sandform is one found in the wake of an immobile object, such as an exposed rock, known as a *sand shadow* (Bagnold, 1941). Sand shadows are formed by deposition of sand in saltation due to localized reduction of shear velocity in the wind shadow of such an immobile object.

Behind any object within a fluid flow, there is a *surface of discontinuity*, outside of which the flow is roughly laminar near the mean wind speed, but inside of which is turbulent, with a mean velocity lower than the mean wind speed. The reason that sand, not dust, is deposited in these areas is a direct consequence of the definition of sand we are using here. While sand is highly influenced by the wind, it will tend to follow a uniform trajectory rather than a changing streamline in the wind. So a grain flying over or around an object while in saltation may, by chance, fall into the wind shadow behind the object, where it will likely stay. A dust grain in suspension, however, will tend to follow the changing streamlines and fly past the wind shadow.

In addition to sand deposits found in the wake, any obstacle will also have a small pile in front of it, due to yet another wind shadow in front.

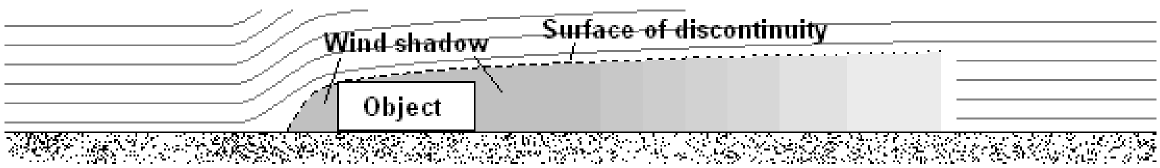

Figure 3: Wind flow around a surface object. Sand will tend to accumulate in the wind shadow, where the wind is turbulent with a lower average speed

A related sand formation is a *sand drift*, which forms in gaps between objects and in wind shadows caused by changes in terrain.

Sand shadows and drifts require the presence of obstacles to alter the boundary layer fluid flow. However, one of the most interesting properties of sand is that a flat sand sheet is unstable under a fluid flow. The mechanism for this peculiar property becomes apparent when you analyze the case of saltation over a flat sheet of sand.

Take the simplifying case of a flat sheet of sand undergoing a uniform barrage of saltating grains. In addition to there being a characteristic path to describe the average path of saltating grains, it turns out that all grains descend at a very uniform angle of descent. Because of this, the descending grains can be represented by parallel vectors, as in Figure 4.

A “flat” sand sheet can not be perfectly flat, as it consists of finite grains of roughly circular proportions. As such, at any moment there exists a multitude of miniscule pits and discontinuities. Figure 4 shows just such a deformation, where a small depression has formed momentarily due to a few saltating grains being removed. Because of the near-uniform descent angle of grains in saltation, the existence of the depression causes more sand grains to impact in the downwind slope of the crater than the upwind slope.

The sand flux due to surface creep, q_c, is proportional to the number of impacts per surface area. Therefore, the downwind side of the temporary depression is suddenly subjected to a much higher sand flux. Since there are now more grains moving out of the depression than into it, a continuous saltation will serve to deepen the depression and extend it downwind.

Figure 4: Differential intensity of saltation bombardment. When a chance depression forms in a sand sheet, ongoing saltation will serve to deepen the depression and extend it downwind

When the sand surface begins to deviate from the ideal flat sand sheet case, the ideal situation seen in Figure 4 with an even distribution of descending grains at a constant angle no longer applies. Knowing that saltating grains have a characteristic path, a grain leaving the sand bed at some point will tend to land very near to a point one saltation length downwind. Therefore, if an area has a much higher sand flux due to increased saltation impacts, the same will apply for an area one saltation length downwind. In this way, a single chance depression will soon become an extended area of *sand ripples*. These sand ripples have a very regular wavelength which is dependant upon the prevailing wind speed, and is remains constant over time as long as the wind speed remains constant.

The shape and height of these ripples depends on the surface sand grading, or the distribution of sand grain size. This can be deduced by a simple analysis of growing ripples: as the height of each ripple increases, the average velocity at the grains will increase according to the boundary-layer wind distribution (Equation 1). If the range of grain sizes in a particular sand bed is small, the higher wind speed at the top of ripples will tend to topple the grains at the crest into the next trough. Therefore a narrower range of grain sizes will result in smaller ripples. A wider range of grain sizes will allow for larger ripples.

As seen previously, an area of increased grain impacts will also see an increase in the grains moved by surface creep. Therefore, if a significant portion of the grains in the sand bed can only move by surface creep, a different kind of sand formation will be seen. In this case, after the initiation of saltation, the smaller grains are slowly removed until the larger grains begin to dominate. Ripple-like formations will still emerge, but they will have essential differences. Larger grains only capable of surface creep will begin collecting at each crest, creating a wind shadow for the subsequent trough similar to that in Figure 4. Since the larger grains are moved much slower than the smaller grains, and cannot move in their own shadow due to a lack of saltation, the collection at each crest grows larger, as shown in Figure 5. These features are known as *ridges*.

At some point, assuming uniform conditions throughout the sand bed, the ridges will grow large enough to shelter the troughs completely, halting saltation, and creating a stable configuration of small, steep-faced ripples. However, a more common case is one where there is an oncoming saltation from upstream. In this scenario, the surface creep will continue to build the ridges higher. With higher ridges, the wind shadows grow longer, and subsequently the wavelength increases. If saltation conditions prevail for long periods, ridges can grow indefinitely. So unlike ripples, the wavelength of ridges does not depend on the mean wind velocity.

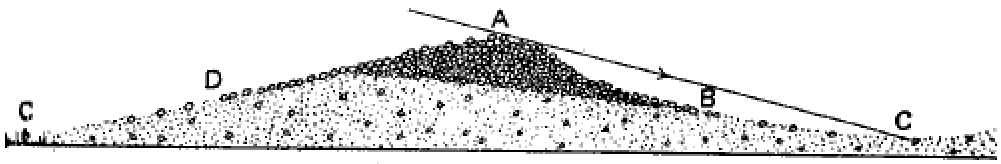

Figure 5: A typical ridge. The line AC represents the wind shadow where no saltation or surface creep is taking place, the line DA is the area of maximum surface creep, and the line AB is where creeping grains from the crest are avalanching down the downwind slope. From Bagnold, 1941.

There is a third feature, known as a *megaripple*, which can form under the same conditions as normal ripples. They are widely spaced, less regular in their repetition than normal ripples. It is unknown whether their wavelengths are dependant upon grain distribution or properties of the local wind regime. Little is known about their genesis or evolution, and many consider them to be dunes rather than ripples or ridges, but they have been widely observed on the surface of Mars.[1]

One important feature distinguishes ripples and ridges from other sand forms. In ripples and ridges, the coarsest grains appear at the crests, with finer grains in the troughs. The opposite is true for so-called *large-scale sand formations,* the majority of which are true *sand dunes*.

4.2 Dune formation

The genesis of dunes has actually been observed only rarely in any detail (Lancaster 1995). Only a few studies have documented properties of dunes from formation until maturity, and these only noted the physical transformation of the dune, not the sand properties believed to be important in dune genesis. The accepted theory regarding dune formation comes mainly from the study of mature dunes and wind tunnel scenarios, so there is an inherent uncertainty in the exact processes which take place.

[1] http://www.tec.army.mil/research/products/desert_guide/lsmsheet/lsgran.htm

Contrary to popular belief, a sandy desert floor on Earth is rarely composed entirely of sand. A typical desert floor is either composed of a sandy surface interspersed with pebbles and a few larger boulders, or what is known as a *desert pavement*, where all surface sand and dust have been removed, leaving a layer of interlocking pebbles.

The desert pavement case is irrelevant for our purposes. In other areas, large pebbles among smaller sand grains will tend to space themselves out evenly, regardless of their initial distribution. Because of this, the presence of pebbles tends to stabilize a sand sheet, halting saltation by raising z_0, the level at which average wind velocity drops to zero. However, if a sand sheet stabilized by pebbles is subjected to a stronger wind, more sand may be removed, until another equilibrium level is reached where the sand grains are sheltered by the pebbles.

A sandy area with large pebbles can sustain a much higher sand flux than a bare sand sheet. This is due to the tendency of saltating grains to rebound higher and longer when impacting an immobile object such as a pebble. So when a patch of bare sand forms by deposition or other processes, the tendency will be for upwind saltation to deposit sand on an existing sand patch. However, a pebbly surface will have a much higher surface roughness than a surface of bare sand, and so the fluid threshold shear velocity will be much higher as well. So if the shear velocity is not much higher than u_{*ft} for the pebbly surface (a "gentle" wind), the sand patch will be stretched downwind and dispersed.

In the case of a shear velocity much higher than both fluid thresholds (around $4\times u_{*ft}$, a "strong" wind), saltation will begin in earnest before the wind reaches the sand patch. At the upwind edge of the sand patch, saltation increases violently, causing substantial drag which causes a reduction in the wind velocity at and just upwind of the bare sand patch, which in turn results in a net deposition of sand. In this way, a strong wind will serve to increase the thickness of a sand patch, as well as extend it upwind. The same process has been shown to occur in areas where the surface roughness changes more gradually, due to a change in the sand grading.

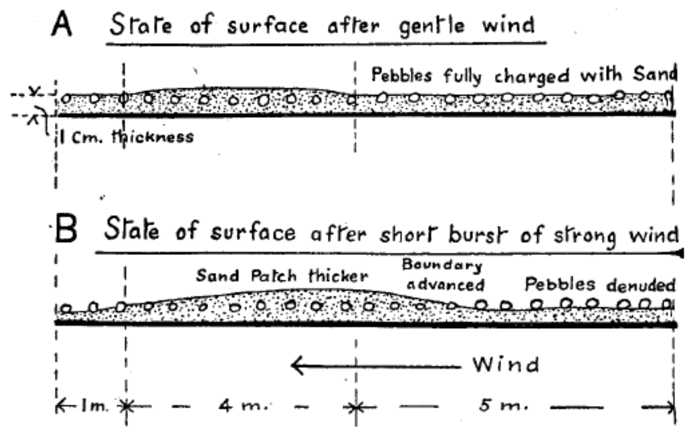

Figure 6: Accretion on a patch of bare sand. From wind tunnel experiments by Bagnold, 1941

In order for dunes to form in these areas of changing surface roughness, four conditions must be satisfied. First, wind which causes saltation along the smoother sand surface must not blow for too long, lest it dissipate the sand accumulation entirely. Second, for the duration that the strong wind blows, there must be a consistent supply of sand from upstream, or else the smoother sand patch will quickly dissipate in much the same manner. Third, there must not be a large amount of grains in surface creep, as these grains will tend to encroach upon the smoother patch of sand, preventing dune growth. Fourth and lastly, the smoother sand must be at least as long as the saturation length, as there will be varying instances of removal and deposition as the new wind profile adjusts. This saturation length, usually between 4 and 6 meters on earth, represents a lower limit for the size of true sand dunes.

There are two mechanisms by which upwind saltation could be sustained. The first case we will consider is a unidirectional wind profile, where both strong and gentle winds blow in the same direction (±15º) (Lancaster, 1995).

In a unidirectional wind regime, any sand patches will have no mechanism by which to become wider, and may only extend in the downwind direction. This leads to the appearance of *sand strips*, which are arranged parallel to the prevailing wind. Unless the wind is much higher than the sand's threshold shear velocity, these sand strips will soon thin out to the point where buried pebbles start to reemerge, in addition to encroaching grains in surface creep. However, if a period of strong winds occurs, an interesting self-sustaining wind regime may form close to the surface. The intense saltation ongoing over the sand strips saturates the boundary layer, slowing the near-surface wind velocity significantly.

The intervening areas between strips are pebbly, and under a gentle wind the higher surface roughness dictates that the near-surface wind velocity will be lower than over the sand strip. This situation changes in the above case of a very strong wind. While there may or may not be saltation over the pebbly surface, the density of saltating grains will be less, assuming the wind is not so strong that this area is saturated as well. This creates alternating streams of slower and faster wind, which tends to create small eddies and vortices, the sum of which is a convergent wind pattern on the sand strips. This process can be seen in Figure 7. If the strong wind can be sustained for a long enough time, these sand strips may eventually build into *longitudinal dunes*, which are arranged parallel to the wind flow.

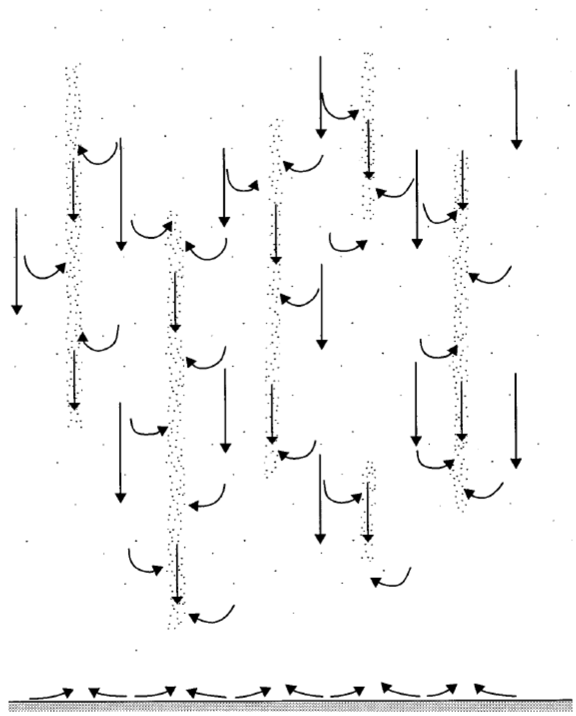

Figure 7: Appearance of longitudinal vortices among sand strips under severe saltation. From Lancaster, 1995.

The second case, where gentle winds blow in a different direction than the stronger winds, is much simpler. If an isolated sand patch is created, a strong wind will build it up, at the expense of a now-denuded area just downwind. If gentle winds occur, just barely above the saltation threshold, from a different direction, they will thin out the accumulated pile slightly, but also replenish the denuded area with a fresh layer of sand. This regime tends to create *oblique* *dunes* or *transverse dunes*, depending on the magnitude of the direction difference. Oblique dunes are arranged at an angle to the direction of dune propagation, while transverse dunes are perpendicular to the direction of dune propagation. Regardless of which case occurs, a continuation of strong winds will build a budding dune steadily up to a certain point. However, when the dune reaches a size where it begins to alter the nearby wind profile, it no longer needs a strong wind to sustain it.

When a dune first forms, a cross-section taken parallel to the dune-building wind typically takes a shape similar to the one shown in Figure 8. Because of the projection of the dune up into the wind stream, the dune significantly alters the wind profile. Closer streamlines on the upwind or *stoss* side of the dune show areas of higher wind velocity, indicative of a net positive sand flux, or sand removal. On the downwind or *lee* side of the dune, the streamlines spread apart, showing an area of net negative sand flux, or sand deposition. In this way, a dune can move essentially unaltered across a desert floor, even if the wind is only strong enough to move the bare sand on the dune.

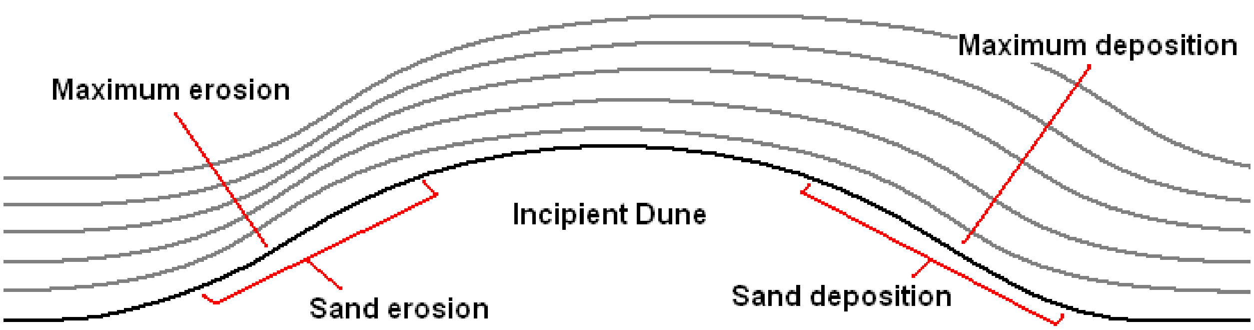

Figure 8: New dune altering the wind profile above itself. The streamlines appear closer together on the stoss side of the developing dune, and further apart on the lee side, so sand is removed from the front of the dune and deposited downwind, causing dune movement.

A sand dune can not remain in this uniform, hill-like profile for long. Equation 9 gives the sand flux on a simple hill-shaped dune undergoing no net flux (Bagnold, 1941).

$$q = cg\rho_s \tan(\alpha)x \qquad 9$$

where x is the horizontal distance from the upwind foot of the dune, c is the velocity of the dune, ρ_s is the density of the sand in bulk (including air between grains), and α is the inclination of the dune surface at point x. Therefore, all other factors being equal, the both the net removal and deposition of sand will occur at the point where the slope is the steepest, shown in Figure 8. With an unequal sand flux, different areas of the dune will begin to advance at different rates, leading to an oversteepening of the lee slope as seen in Figure 9.

When sand is piled on itself, like any granular material, it can only support itself against the force of gravity to a certain point. Because of frictional and inter-grain cohesive forces, a sand pile can achieve a fairly large angle, typically around 34° for sand on Earth. Any slope steeper than this angle will collapse, avalanching until the slope below this critical angle, known as the *angle of repose*. In the case of a moving dune, sand avalanching in this manner will eventually morph the lee slope into a fairly straight slope just shallower than the angle of repose. This straight slope is known as a *slip face*, and is always roughly transverse to the direction of winds above the saltation threshold.

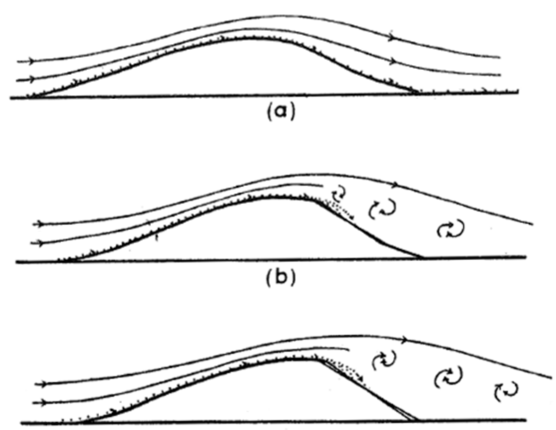

Image from Bagnold, 1941

Figure 9: Development of a slip face. In (a), the lee slope has steepened to the angle of repose, and additional deposition at the dune crest causes sand to begin avalanching down the slope (b) , creating a slip face. As the dune advances, deposition continues to occur at the dune crest, but stops at the foot of the dune, maintaining the entire slope as a slip face

With the formation of the slip face, the lee of the dune now contains a wind shadow, with a surface of discontinuity roughly equal to the surface of the ideal "sand hill" shown in Figure 8. The wind shadow will serve to increase deposition even further at the foot of the dune, causing dunes with slip faces to continue to grow. The dune has now reached maturity, and will continue to evolve and migrate as long as there is a consistent wind above the saltation threshold.

4.3 Dune types

The exact evolution of the dune beyond its initial formation depends upon two factors: the amount of sand available for saltation outside of the dune, and the wind regime complexity. The previous descriptions of dunes as, longitudinal, oblique, or transverse refers only to the arrangement of individual dunes in a group in reference to the prevailing wind regime. These terms have little or no bearing on the actual dune type. There are three major types of dunes, each of which represents different local conditions, and, most importantly, *all of which* are found on Mars (Lancaster, 1995).

The first dune type, arguably the easiest to recognize, is the *barchan dune*. Barchans form in areas of limited sand availability and unidirectional wind regimes. The stoss side of the dune is relatively featureless and dome-shaped. The slip face is curved, resembling a bite which has been taken out of a dome-shaped dune, terminating with two *horns* extending downwind, one on each side of the dune.

Now, the curved slip face is not an indication of changing wind directions. It is a consequence of the change in sand-wind interaction as the dune grows. A larger dune begins to interrupt the linear fluid flow, causing it to curve slightly around both sides of the dune. Since the local wind speed is the most important factor in determining the slip-face orientation, this slight curvature of the horizontal wind profile causes the slip-face to become curved (Bagnold, 1941).

Figure 10 shows a very neat example of a Martian barchan dune. This dune exists near 41.4°S 44.6°E, on the western rim of Hellas Basin, the largest impact crater on Mars, and is part of a chain of barchans not seen to the lower left and upper right. In this image, by the Mars Reconnaissance Orbiter's HiRISE imager, all the classic barchan features are visible. The curved, crescent-shaped slip face is prominently featured in the center, dissipating into two "horns" downwind. The remainder of the dome-shaped dune is covered in sand ripples, which tend to form on barchans due to their unidirectional wind environment. The dune-forming wind is from ENE-to-WSW, and the ground outside of the dune is a jumbled bedrock terrain, distributed with small sand deposits, suggesting very limited sand availability. The dune is about 120 m long from stoss foot to horn tip, with the horn-to-horn distance of about 40 m, fairly typical of large barchans found on Earth.

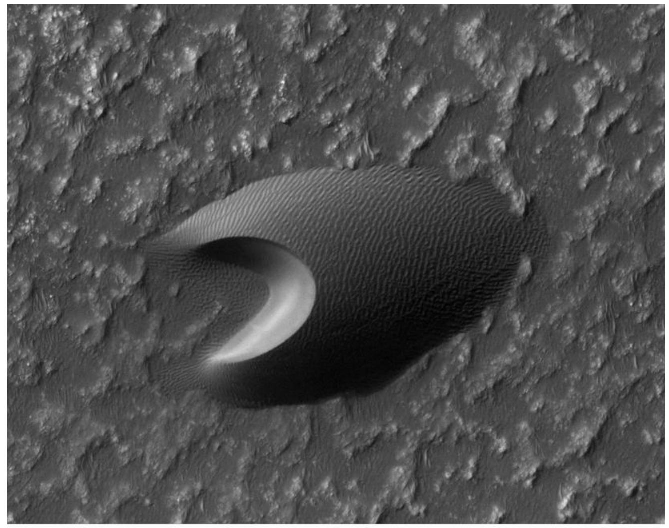
Figure 10: Barchan on west rim of Hellas Basin, Mars

The barchan is one type of the larger group of *crescentic dunes*, all of which are formed under unidirectional wind regimes. Another type of crescentic dunes is very closely related, *crescentic ridges* (not actual ridges, but a type of dune). Crescentic ridges resemble parallel chains of barchan dunes which tend to overlap. Logically, crescentic ridges form in areas where sand availability is higher than with pure barchans, but the wind regime is still unidirectional (Lancaster, 1995)

On earth, the most common type of dune is the *linear dune*. However, on Mars, linear dunes only appear to be dominant in about 5% of large dune fields (Hayward et al., 2007). Linear dunes appear when there are two dominant sand-moving directions, separated by more than 15º. (Lancaster, 1995) The slip face is not fixed with respect to a linear dune, but shifts from one side of the crest to the other as the wind regime changes. A related dune type which has also been found on Mars is the *reversing dune*, which is formed by a wind regime which periodically changes direction close to 180º.

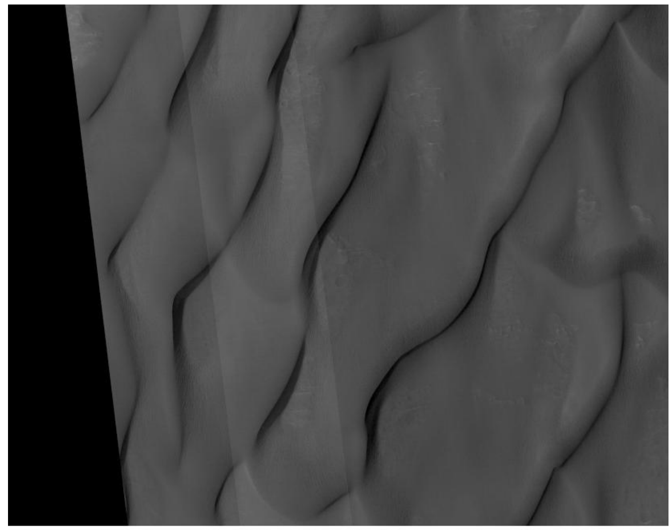

Figure 11: Linear dunes near Gale Crater, Mars

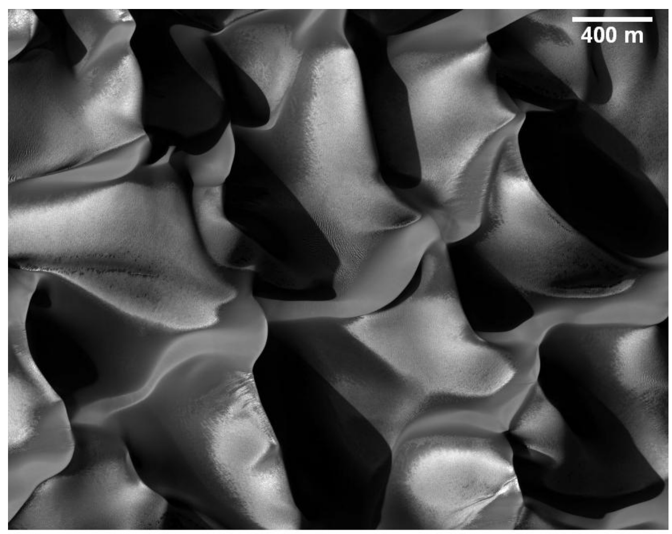

Figure 12: Star dunes in Proctor Crater

An even more complicated wind regime, featuring three or more prominent wind directions, results in the formation of *star dunes*. These can be the largest dunes, building to several hundred meters high on Earth. These dunes have multiple slip faces, which are active and inactive depending on the current direction of the wind. On Mars, they are often found on the floor of smaller craters such as Victoria Crater.

5 Expected nature of sand-surface interaction on Mars

5.1 Martian weather and climate

Mars has long been theorized to have an active atmosphere, possessing many of the familiar transient atmospheric characteristics which we on Earth call “weather”. As early as 1877, Giovanni Virginio Schiaparelli observed what he thought were “clouds” in the Martian sky (Parteli, 2007). While it is almost certain that what he observed were *dust storms* which cover the surface of Mars every year or so, it began the race to determine just how “alive” the Martian atmosphere currently is.

Mariner 9 offered the first up-close look at the planet and its atmosphere in 1971. Imagery at Mariner 9’s arrival indicated that Mars was in the midst of a planet-wide dust storm, obscuring the surface to the point that the striking polar ice caps were not even visible (Parteli, 2007).

After a few weeks, the dust storm cleared, allowing for the first clear, high-resolution images of the Martian surface. These images clearly showed large expanses of dune fields on all corners of the planet. This spurred theories of an active atmosphere with ongoing sand movement.

Five years later, the *Viking* landers reached the surface of Mars, taking the first direct measurements of wind speed in an extraterrestrial environment. They measured a mean wind speed which rarely exceeded 10 m/s, which corresponds to a wind shear velocity of approximately 0.8 m/s, assuming several theoretical values are correct (Moore, 1985). These wind measurements were only taken at one height (1.6 m), so the typical wind *profile* on Mars could still only be estimated.

There were several significant dust storms during the *Viking* missions, each of which was associated with a peak in wind speeds to 20 m/s or more. In at least one case, the wind reached 40-50 m/s (wind shear velocity 3-4 m/s) for a period of around 40 seconds at the *Viking 1* lander, causing the first observed saltation event on Mars.

The *Pathfinder* rover, *Sojourner*, contained instruments to gather this missing data. The Pathfinder landing site (19.33 N, 33.55 W) was not far from the *Viking* 1 site (22.697° N latitude and 48.222° W longitude), and in an area of similar surface composition (Sullivan, 2002). *Sojourner* featured a meteorological boom with three wind socks, which was to help fill in the missing data. Unfortunately for the meteorological goals of the mission (although probably fortunately for the mission in general), the weather was calm for the entire 83 Martian-day mission, with the wind never climbing above 10 m/s at the 1 meter elevation, and no observed sand or dust movement (Sullivan et al., 2000; Sullivan 2002). There was enough data to estimate a fluid threshold shear velocity of 4.5 m/s, much higher than the numerically and experimentally predicted value of 2.0-2.5 m/s, likely due to the abundance of boulders and large rocks (Sullivan, 2002).

Thus it is expected that the average weather on Mars is relatively calm. However, during dust storms, it appears that winds above the saltation threshold can occur, and have occurred in the past. These planet-wide dust storms occur almost every year in the Martian northern-hemisphere autumn, and likely happen with such repetition because the atmospheric pressure is highest at that time (Larsen et al., 2002).

Temperature at the surface has only a minor influence on saltation, aside from possibly preventing it in the case where water or CO_2 frost accumulates. Temperature has been found to vary widely with season, latitude, and time of day, just as on Earth, but typically is in the range of 180-260 K (-135ºF to 10ºF) in the summer and 160-200 K (-170ºF to -100ºF) in the winter.

5.2 Global distribution of sand dunes and sheets on Mars

Although aeolian processes are ubiquitous on Mars, large-scale sand sheets/seas, dune fields and ergs are not as extensive on Mars as on Earth. A recent estimate of the coverage of large-scale sand features (dune fields and sand sheets) on Mars is on the order of 800,000 km^2, or about 1% of the Martian surface surveyed in that study (Hayward et al., 2007). On Earth, large-scale sand features cover approximately 5,000,000 km^2, and while this is 1.0% of the Earth's total surface area, it is 3.4% of Earth's land area.

On Mars, dunes are found almost exclusively within craters and Valles Marineris, the 4000 km-long canyon system near the planet's equator. While on Earth most dunes are linear in nature, on Mars a vast majority of dunes are crescentic, with a smaller amount being linear (Hayward et al., 2007). Large dune fields feature very few star dunes; however, smaller dune fields in medium-sized craters almost universally have a star-like appearance.

As aeolian processes seem to be the only active geological processes on Mars, aside from impact craters and very localized water action, the lower concentration of dunes compared to Earth suggests that there is less sand available for saltation, either because winds above the saltation threshold are less prevalent or there is less total sand on Mars. Indeed, it may be a combination of the two. The main source of erosion which produces sand-sized particles on

Earth is oceans and other hydrological processes; these are obviously absent from present-day Mars. On top of that, evidence for present-day winds above the saltation threshold is very sparse. Prior to the landing of the Mars Exploration Rovers, there has only been one verified instance of indirectly observed saltation on Mars, during the (*Viking 1*) Martian Dust Storm of Sol 1742 (Moore, 1985).

5.3 Properties of the surface and atmosphere at Meridiani Planum

While the initial scope of this study was a planet-wide search for dune movement, eventually the search for directly-observed movement of sand moved to Meridiani Planum, in the area around Victoria Crater, where Mars Exploration Rover *Opportunity* has been aggressively imaging the landscape.

Wind data is sparse for the Martian surface. Only three landers have succeeded in making wind measurements, and only the two *Viking* landers have a data set more than a few months long. However, these data sets agreed that the shear velocity rarely exceeds 1.0 m/s, and only dust storms contain winds strong enough to produce saltation. This is much lower than u_{*ft}, which is estimated to be approximately 2.0 m/s at Meridiani Planum (Sullivan et al., 2005).

For the area of Meridiani Planum, as with most of the surface of Mars, the sand is composed of basaltic sandstone.[2] The grains are approximately 50-150μm in diameter, topped by a scattering of pebbles as large as a few millimeters. The density of grains has been estimated as approximately 3200 kg/m^3 (Sullivan et al., 2005).

[2] http://erc.arc.nasa.gov/MarsVolc/basalt.htm

Like Earth, the wind is rarely dead calm on Mars. This is apparent from wind speed measurements by both *Viking* landers and *Sojourner* rover, which were typically less than 10 m/s (22 mph), but were rarely dead calm. At Meridiani Planum, prevailing winds during apparently calm weather gradually removed dust from *Opportunity*'s solar panels over a period of 50 Martian days in the summer of 2006.

5.4 Expectations for sand dune movement on Mars

Many studies have attempted to find conclusive evidence of sand movement on Mars. It is apparent that dunes are either migrating very slowly now, or have migrated in the recent past. There are two main bodies of evidence which support this: first, there are *very* few known impact craters on dunes, and second, most Martian dunes appear crisp, with well-defined slip faces. Studies have estimated that, if sand movement does occur, it is at a rate of 1-8 cm per year at most (Fenton, 2006).

Dune fields at Rabe Crater (44 ºS, 35ºE) and Proctor Crater (48ºS, 30ºE) have shown strong evidence for dune movement. Images of Rabe Crater dunes show alternating dark and light streaks on the dunes' slip faces which change even over the course of a single Martian year, which have been interpreted as saltation-induced grainflows (Fenton, 2006). Images of Proctor Crater dunes indicate possible slip face reversing on barchanoid dunes (Fenton et al., 2005). There is even a suggestion in this study that one slip face moved as much as 37 m, however, I believe this is more likely attributable to frost and/or dust changes. No study has yet succeeded in directly imaging a change in dune position, which would confirm dune migration.

6. Observation techniques

6.1 History of early observations of Mars

Mars is a prominent visible feature in the night sky. At its closest approach to Earth, it is the 4th brightest object in the night sky, and one of the only visible objects to be bright red. As such, it has been observed since man first gazed upward, and was recorded by many ancient civilizations as a star signifying war or death. Until the 17th century, however, it was merely a mote of red light, varying in brightness over the period of a few years.

The first observations or recognizable features on the planet's surface are attributable to Christiaan Huygens, who sketched a dark plain now known as Syrtis Major, as well as the bright southern polar ice cap, in 1672. In the same year, Giovanni Domenico Cassini observed a transit of a small star by Mars, and concluded that it must have a very thick atmosphere; although it turned out that his observations were flawed, this was the first "evidence" of a dynamic Martian atmosphere. In the early 18th century, Giacomo Filippo Maraldi drew what he thought were clouds stretched across the planet, though these turned out to be permanent features of the planets surface which are still visible today. He also described changes he observed in the southern ice cap, and suggested that the properties of the surface there changed somehow from year to year (Sheehan, 1996).

In 1783, William Herschel observed another Martian transit and concluded that Cassini's observations of a very thick Martian atmosphere were false. However, he also observed what he called "occasional changes of partial bright belts", concluding they were storm clouds above the planet. As the few clouds known to exist on Mars are not visible even today from Earth, Herschel likely was observing local dust storms. In the 1820s and 1830s, Johann Heinrich Mädler and Wilhelm Beer made many contributions to the study of Mars, conclusively proving that the previously observed dark patches were permanent surface features, and determining the planet's rotational period to within a few seconds. In 1837 they observed that Mars was nearly featureless save the ice caps, possibly indicating the first observation of a planet-wide dust storm. In 1864, Rev. William Rutter Dawes improved greatly upon Mädler and Beer's observations, making drawings depicting almost every major albedo feature identified today (Sheehan, 1996).

At this point, there was little more that could be learned from earth-bound telescopes, given the limitations imposed by atmospheric aberrations. In fact, further refinement of observations, more often than not, were completely wrong. In the 1870's, Giovanni Virginio Schiaparelli first made the infamous claims of *canali*, Italian for "canals" or "channels", on the surface of Mars. As it turned out, the "channels" were either illusions due to optical effects, or simply imagined features (Sheehan, 1996). Until the 1960s, the prominent theory was that the dark albedo features on Mars were swaths of vegetation, and the ice caps were seasonal patches of water-ice (Sheehan, 1996). There were observations of yellow clouds, thought to be dust storms, and white clouds, thought to be analogous to earthbound clouds. There was even a scientific consensus that many dark features were blue in color (Sagan and Kellogg 1963).

However, there were some doubters to the scientific consensus. Some theorized a desert-like planet with large dune fields and no vegetation. As early as the 1950s the idea of a Martian surface dominated by sand dunes was proposed (Gifford, 1964). A few scientists also doubted the existence of the *canali* as anything more than mere optical illusions.

6.2 Observations from Martian probes.

Those doubters were proven right by the observations of *Mariner 4* in 1965. Sending spacecraft to Mars was no small task—several probes launched by both Russia and the United States failed to reach Mars successfully in early 1963 and mid-1965. *Mariner 4* performed the first successful fly-by of Mars in July, 1965. It was only able to take 22 discontinuous, low-resolution, blurry images, but they were sufficient to reveal that the traditional view of Mars's atmosphere was quite wrong. The images taken by the television camera revealed an old, dry, cratered surface, with no canals, no vegetation, and no evidence of life whatsoever. Indeed, it looked closer in appearance to the moon than to Earth. To further disprove the contemporary theories, atmospheric measurements indicated that the surface pressure was at most a few millibars, and was composed almost entirely of carbon dioxide (Sheehan, 1996).

It was at this time that the idea of dust storms as the main form of weather on the planet first rose to prominence. It was the only plausible explanation for the seasonal changes in albedo features, with the idea of liquid water and vegetation now all but debunked. The images were not nearly detailed enough to image sand dunes, however, it was widely believed that the atmospheric dust was lifted by surface sand movement and saltation impacts (Goody, 1969).

The next probes sent to Mars, *Mariner 6* and *Mariner 7*, would add detail to the planets surface (high-resolution imagery of about 10% of the planet's surface), and confirm the atmospheric measurements made by *Mariner 4*. By chance, they photographed no dust storms or dune fields, especially because only a few dozen images from these two probes were of high enough resolution. However, they did capture images of frost in craters, as well as confirm that the ice caps were likely CO_2 ice (Sheehan, 1996).

The next successful mission, *Mariner 9*, was also the first successful Mars orbiter. In fall of 1971, it began returning images of a planet completely devoid of surface features. After shutting down for a month to conserve power, it began returning images rich in detail, including craters, valleys, and, most importantly, sand dunes. *Mariner 9* was able to image most of the surface down to a resolution of 100 meters or so.

Since then, the resolution of images sent back from Mars has steadily improved. In the late 1970s and early 1980s, the *Viking* orbiters imaged much of the planet down to a resolution of 40-90 meters, with many areas of interest imaged as well as 10-meter resolution. The next Mars orbiter, the Mars Global Surveyor, arrived almost 20 years later in 1997. It's Mars Orbiter Camera imaged about 70% of the planet to better than 7-meter resolution in almost 10 years orbiting Mars. Finally, the current Mars Reconnaissance Orbiter's HiRISE camera is imaging areas of interest with a resolution of 25-50 centimeters.

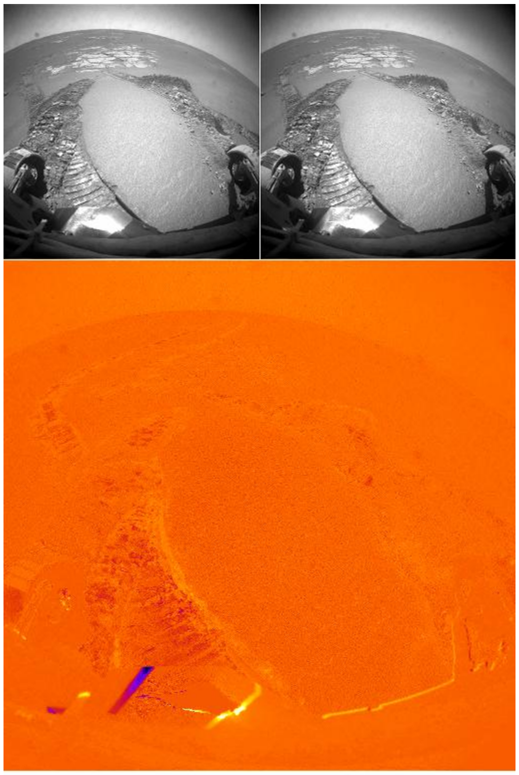

Figure 13: Photo-comparison with ImageJ. The bottom plot measures the difference between the first two pictures, pixel by pixel. The minor dark and light streaks at the bottom of the photos are major changes, but clearly due to changing shadows, due to the images being taken at different times of day

6.3 Methodology for image comparison

The backbone of this project was interpreting changes in images from one scene to another. This was often done visually: making a digital slide show of a sequence of images and cycling through to spot changes. Indeed, this was often the only feasible method for comparing most satellite images, as they were often taken from greatly different orbital angles. This meant that images of the same 3-dimensional scene could be distorted based on the observation angle, which would take a great deal of complicated processing, far beyond the abilities of this project, to compare digitally.

However, for surface images of particular interest, a Java-based image processing program called ImageJ was used. ImageJ allowed for a pixel-by-pixel comparison of the images, mapping the differences as shown at right. The result was an image where major changes were highlighted, an example of which is shown in Figure 13.

7. Observations of dunes from orbiters

7.1 Observations to be used in this initial study

Initially, this project was to make use of imagery from Mars orbiters to detect dune movement on the surface. Even with large amounts *in situ* imagery from two fixed landers and three rovers, imagery on the scale of 0.1 meters or less covers far less than 1% of the planet's surface. By contrast, almost 100% of the planet's surface has been imaged to a resolution of at least few dozen meters. With such a large data set available (over 800,000 km^2 of dune fields larger than a square kilometer), many of which were imaged repeatedly by high-resolution cameras over more than a decade, it seemed quite a reasonable goal to find dune movement solely through orbital images.

Dune fields at Rabe Crater (44 ºS, 35ºE) and Proctor Crater (48ºS, 30ºE) were chosen for the initial observations because they were the focus of previous studies which found strong evidence for dune movement. Images of Rabe Crater dunes show alternating dark and light streaks on the dunes' slip faces which change even over the course of a single Martian year, which have been interpreted as saltation-induced grainflows. (Fenton, 2006) Images of Proctor Crater dunes indicate possible slip face reversing on barchanoid dunes. (Fenton et al., 2005) There is even a suggestion in this study that one slip face moved as much as 37 m, however, I believe this is more likely attributable to frost and/or dust changes.

The first image set analyzed was images taken by the Thermal Emission Imaging System (THEMIS) visible camera aboard the 2001 Mars Odyssey orbiter. This imager was chosen due to its greater coverage of the surface (~80%) and consistent image resolution, due to it having a very low orbital eccentricity (0.0115).

The next image set analyzed was from the Mars Global Surveyor's Mars Orbiter Camera (MOC), and showed much more promise. There was a large set of images, some with resolutions of better than 1.5 meters, taken over a period of 5 Martian years. This was the data set used in most previous dune movement studies. A third data set, studied concurrently with the MOC images, was from the newest addition to Mars' orbit, the Mars Reconnaissance Orbiter's High Resolution Imaging Science Experiment (HiRISE), which has a consistent resolution of approximately 0.3 meters.

7.2 Absence of dune movement visible from orbit

It quickly became clear the resolution of the THEMIS visible camera was highly insufficient for this study. While the image coverage was ideal, with many areas imaged several times over the course of 3 Martian years, the resolution of 18 m (at best) was at least an order of magnitude too large to detect any predicted dune migration.

The other two orbiters showed some initial promise. However, after studying dunes in Rabe and Proctor craters, as well as a few additional sites, including Victoria Crater, I concluded that the original scope of my project, a search for direct observation of Martian dune movement from orbit, was not feasible with the present data set. Some of the images compared can be found in Appendix 1.

The resolution needed to discern the predicted motion of sand dunes on Mars is simply not met by the images currently available, as can be seen in Table 1. It is apparent that among the many Martian orbiters over the years, and the many cameras aboard these orbiters, only the MRO's HiRISE camera will be feasible for directly imaging sand dune movement, and that this will not be possible for at least another few years with proper repetition of images.

Probe	Year	Resolution (m)	Res. Velocity (m/Myr)
Mariner 9 Camera	1972	100	5.22
Viking 1 Orbiter Camera	1976	10	0.59
Viking 2 Orbiter Camera	1976	10	0.59
Mars Global Surveyor MOC	1997	1.5	0.26
Mars Odyssey THEMIS	2001	18	4.83
Mars Recon. Orbiter HiRISE	2006	0.3	0.28

Table 1: Resolution of visible cameras aboard Mars orbiters. The resolution velocity is each camera's maximum resolution in meters divided by the number of years since the first pictures were taken, giving a rough measure of the minimum rate of change visible by each camera's image set, in meters per Martian year

8. Observations from Mars Exploration Rover *Opportunity*

Once the infeasibility of detecting dune movement from orbit became apparent, I searched for an alternate way to produce results. I decided to change my aim to search for saltation and/or dune movement using imagery from Mars Exploration Rover *Opportunity*.

8.1 *Opportunity*'s landing

Opportunity landed successfully on Mars on January 25, 2004 at coordinates 1.94° S, 354.47° E (planetocentric coordinates). Since the 24.6 hour Mars days do not correspond to Earth days, a calendar of numbered Sols has been adapted for all surface-based Mars missions. Thus, for the *Opportunity* mission, January 25, 2004 was Sol 1.

The method for landing the rover safely was the same as for its sister craft, *Spirit*. The rover was transported to Mars within an aeroshell, consisting of a heat shield for atmospheric entry and a "backshell" (JPL, 2007). After a certain time, a parachute opened to begin decelerating the rover. Retro-rockets were then fired, slowing the rover's descent enough to safely deploy the final breaking mechanism, the airbags.

Opportunity and its lander, after bouncing dozens of times, landed in the center of a small 20-meter-diameter crater designated Eagle crater. It was not long before surprises about the nature of sand and its transportation began pouring in.

8.2 Initial aeolian observations

8.2.1 Sandforms

Even on Sol 1, some images were returned showing aeolian formations near the rover. The marks from the bouncing airbags introduced a lot of noise, obscuring what ripples, streaks, or other sand and dust features may have existed in the immediate area around the lander. However, a few areas imaged showed clear sand ripples on the southwest side of Eagle crater, as can be seen in Figure 14.

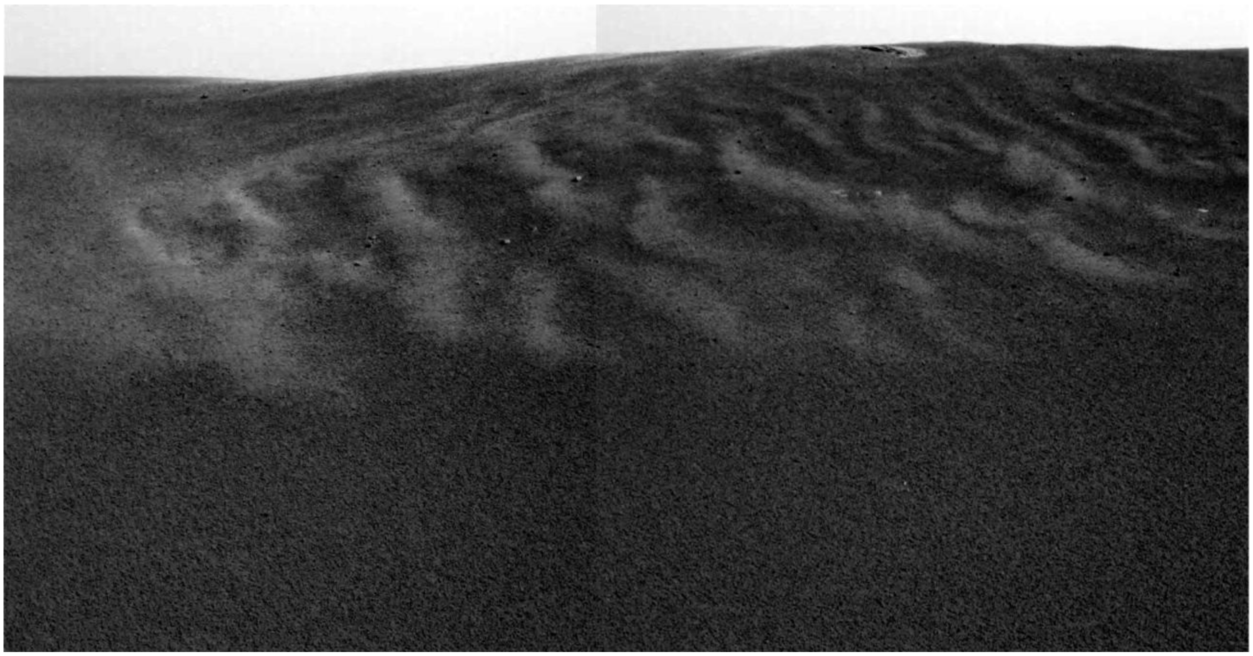

Figure 14: A composite of two photographs taken by *Opportunity*'s Panoramic Camera on Sol 1, showing a clear pattern of ripples on the side of Eagle Crater. The ripples in this image have an approximate wavelength of 0.5 to 1.0 meters.

Subsequent operations included *Opportunity* climbing out of Eagle crater, traveling approximately 750 meters east into and then out of Endurance crater, and traveling more than 7 km south to Victoria crater, which it is currently attempting to enter. In that time, it traveled through flat plains, observing ripples, ridges, and strange pits which appeared to be due to the topography of the underlying bedrock.[3] Between Endurance and Victoria craters, *Opportunity*

[3] http://marsrovers.jpl.nasa.gov/mission/status_opportunityAll_2005.html

visited several smaller craters, some of which contained ripples and ridges. The rover traveled through an extensive field of megaripples several kilometers long, as well as some rocky areas which mainly appeared near the smaller craters.

8.2.1 Observed grain diameters

Martian sand in the area around Opportunity rover, excluding the interior of larger craters, is characterized by fine grains stabilized by a near-uniform distribution of pebbles. These pebbles are almost certainly the stabilizing mechanism which prevents dune formation in this area, assuming saltation-strength winds do occur. However, most inter-crater areas do exhibit ripples and/or ridges, and there is an area of "megaripples", which resemble incipient dunes.

The microscopic imager (MI) on *Opportunity* is a "fixed focus" camera. Because of this, multiple images must be taken at slightly different heights to achieve an in-focus image. Additionally, any in-focus image (or object within an image) must be the same distance from the camera, making the microscopic imager very useful in determining sizes of sand grains and pebbles.

On Sol 10, the MI imaged sand on the floor of Eagle crater, which was mainly sand 50-200μm in diameter, with a few pebbles 1-4mm in diameter scattered about. On Sol 73, it took two sets of images. One set was of the crest of a ridge, the other was of the surrounding inter-ridge sand. The results conformed to the expected grain distribution for a true ripple: The crest was primarily a collection of large grains/pebbles, 0.75-2.0mm in diameter, presumably collected by surface creep processes. The inter-ridge sand, on the other hand, was similar to the grain distribution in Eagle crater, with a few more pebbles. (These images can be seen in Appendix 2) These observations coincide fairly well with conclusions reached in previous studies of *Opportunity* data (Sullivan et al., 2005).

In addition, while previous studies had voiced some doubts (Sullivan, et al. 2005), it appears that the expected *optimum grain diameter* (the particle diameter with the lowest saltation threshold) is well within the range of grains sizes of the sand which appears at Meridiani Planum. The optimum grain diameter was predicted to be around 115μm by wind tunnel experiments, and 150μm by calculations (Greeley et al., 1983; Iverson et al., 1976).

8.3 Unsuccessful attempts at detecting saltation

An attempt was made to survey imagery of all æolian features along the way, and particular attention was paid to images where the rover did not move for an extended period of time. In this way, scenes could easily be contrasted over a long period of time, allowing subtle changes in the landscape to be detected. Imagery was also analyzed from minor dust storms which occurred on Sol 329 and Sols 628-629, with negative results.

The first extended stop *Opportunity* was forced to make began on Sol 446. The rover had been scheduled to make a long drive of 90 meters, but it stopped after only 40 meters after becoming stuck in a small dune or megaripple, later nicknamed “Purgatory Dune”. While engineers devised methods for dislodging *Opportunity* from the dune, the rover continued to take images, allowing for excellent day-to-day comparison of the surrounding sandforms. The most promising target for a saltation search was *Opportunity*’s own tire tracks, which offered an easy view if saltation would occur.

Unfortunately, the few visible changes could be explained by minor dust deposition and frost sublimation, due to images being taken at different times of day. Additionally, it appears that the megaripples are petrified relics of an old wind regime. The sand in this area is encrusted with some sort of conglomerated material, which was disturbed when the rover's wheels passed by and left in blocky chunks near the tire tracks.

After the minor dust storm of Sols 628-629, Meridiani Planum enjoyed relatively good weather. *Opportunity* stuck itself in a megaripple again on Sol 833, this one nicknamed "Jammerbugt", but was able to extract itself after a few days, partly because of lessons learned from Purgatory, and partly because it was not buried as deeply. Image analysis of Sols 833-836 (when *Opportunity* began moving again) again produced no evidence for saltation.

9. "Victoria Rim" dust storm

9.1 Surface observations

On Sol 1232, *Opportunity* drove a few meters, took some images, and shut down. Over the past few Sols, the amount of power produced by the solar panels had been steadily decreasing. More than 99% of the Sun's light was blocked by the atmospheric dust for several days. The electricity production of *Opportunity*'s solar panels, which had been as high as 700 watt hours per day, dropped as low as 128 watt hours, forcing the suspension of regular communications with Earth for the first time (Mars Daily, 2007). Between Sols 1232 and 1254, *Opportunity* could only take a few low-resolution images of the sun and the horizon to measure atmospheric opacity. Between Sols 1235 and 1243, *Opportunity* did not have enough power take any images at all! Luckily, after a few days, the atmosphere began to clear, and power levels began to rise, and the rover resumed normal driving and scientific operations by Sol 1271.

During this intense storm, a major transportation of sediment took place. A side-by-side comparison of images taken on Sol 1232 and 1254 by the right-front Hazard Avoidance Camera (HAZCAM) shows clear differences attributable to a saltation event at some point during the storm. These images appear at full-resolution in Appendix 3.

The second difference, and much more solid evidence of saltation, is the apparent unearthing of new pebbles in the area just in front of the camera. The distribution of pebbles on the sand surface has not changed, but new pebbles have been unearthed, some of them completely. Unfortunately the microscopic imager suffered contamination by dust, so it was unable to image the surface directly after the storm. However, images taken on Sol 1216 show that the sediment nearby was much the same as that seen at the beginning of *Opportunity*'s mission: millimeter-scale pebbles scattered over 50-200µm sand. This suggests the removal of 1-4 mm of sand from this area during the storm.

If the dark areas/deposits seen in the rover's wheels can be proven to be sand, this will prove that saltation occurred during the Victoria Rim dust storm. While at first glance they appear to be shadows, this can not be true. They did not appear in images before the dust storm, are at differing angles to each other, and

Figure 15: Images of sand in rover's wheel

remain fixed in images after Sol 1254, despite those images being taken at different times of day. It is only after the rover begins moving again on Sol 1271 that they disappear. Images of the right wheel can be seen in Figure 15.

Another possible explanation is that the deposit in the shelter of the rover's hollow tires is not a sand shadow, but rather a deposit of dust. This seems feasible until you consider two facts. First, dust is much more susceptible to eddies than sand is, and will tend not to accumulate in stagnant areas merely because it tends to stay in the wind stream. Second, the dust storm was still ongoing for many days after the Sol 1254 image, as evidenced by measures of atmospheric opacity of around 3.7 from Sols 1256-1265. If the deposit had been dust and not sand, it would have undoubtedly changed somewhat between sols 1254 and 1271.

9.2 Supplemental observations

The Victoria Rim dust storm was possibly the most intense storm ever observed from the surface of Mars. *Spirit* rover, on the other side of the planet, imaged the formation and migration of ripples over the course of the storm. HiRISE images from before and after the storm show drastic changes visible from orbit, including the obliteration of *Opportunity*'s tire tracks, and the complete reversal of dust tails trailing from Victoria crater. The dunes in the center of Victoria, unfortunately, showed no apparent movement or deformation in any direction. Images from before and after the storm can be seen in Appendix 1.

10. Conclusions

The evidence garnered and conclusions reached in this study fall short of the ultimate goal of finding conclusive migration of sand dunes on Mars. Sand movement and saltation have been conclusively shown to occur on the present Martian surface, both at the *Viking 1* Lander site (in previous studies) and the Mars Exploration Rover *Opportunity* site. Unfortunately, even with *Opportunity* in such close proximity to the Victoria crater dune field during the saltation event, there was no visible evidence from satellite pictures that the dunes moved at all.

The crucial aspect hindering the detection of dune movement so far is the quality and timescale of the available data. Image resolution has only recently increased to resolving movement of less than a meter, so additional imagery over the next few years should be able to detect any dune movement greater than a few centimeters per Martian year. Also, if *Opportunity* rover is able to continue functioning long enough, it may eventually directly study those dunes, allowing dune movement, if it still exists in that area, to be directly measured for the first time.

11. References

Alghamdi, A. A. A. and Akyurt, M. (2001) "On sandstorms and energy recovery from sandstorms" *Energy Conversion and Management* Volume 42, Issue 9, Pages 1143-1156

AMS. (2000) "Glossary of Meteorology" *American Meteorological Society*. <http://amsglossary.allenpress.com/glossary/search?id=von-karman-s-constant1>

Bagnold, Ralph A. (1941) "The Physics of Blown Sand and Desert Dunes" Methuen & Co. Ltd. London

Bush, George W. (2004) "A Renewed Spirit of Discovery: The President's Vision for U.S. Space Exploration" <http://www.whitehouse.gov/space/renewed_spirit.pdf>

Fenton, Lori K.; Toigo, Anthony D.; and Richardson, Mark I. (2005) "Aeolian processes in Proctor Crater on Mars: Mesoscale modeling of dune-forming winds" *Journal of Geophysical Research* Vol. 110, E06005

Fenton, Lori K. (2006) "Dune migration and slip face advancement in the Rabe Crater dune field, Mars" *Geophysical Research Letters* Vol. 33, L20201

Gifford, F. A., Jr. (1964) "The Martian Canals According to a Purely Aeolian Hypothesis" *Icarus* Vol. 3, pp. 130-135

Goody, Richard. (1969) "Motions of Planetary Atmospheres" *Annual Review of Astronomy and Astrophysics*

Greeley, R.; Williams, S. H.; and Marshall, J. R. (1983) "Velocities of windblown particles in saltation: Preliminary laboratory and field measurements" *Developments in Sedimentology: Eolian Sediments and Processes*

Hayward, Rosalyn K., K. F. Mullins, L. K. Fenton, T. M. Hare, T. N. Titus, M. C. Bourke, A. Colaprete, and P. R. Christensen. (2007) "Mars Global Digital Dune Database and initial science results" *Journal of Geophysical Research* Vol. 112, E11007,

Iverson, J. D.; Greeley, R.; and Pollack, J. B. (1976) "Windblown Dust on Earth, Mars, and Venus" *Journal of the Atmospheric Sciences* Volume 33, Issue 12

Jones, D. K. C. (2001) "Blowing sand and dust hazard, Tabuk, Saudi Arabia" *Geological Society, London, Engineering Geology Special Publications*; v. 18; p. 171-180

JPL. (2007) "Spacecraft: Aeroshell" *Mars Exploration Rover Mission*. <http://marsrovers.jpl.nasa.gov/mission/spacecraft_edl_aeroshell.html>

Lancaster, Nicholas. (1995) "Geomorphology of Desert Dunes" Routledge. New York

Larsen, S. E., H. E. Jørgensen, L. Landberg, and J. E. Tillman. (2002) "Aspects of the Atmospheric Surface Layers on Mars and Earth" *Boundary-Layer Meteorology* Vol. 105, pp. 451-470

Mars Daily. (2007) "Mars Rovers Brave Dust Storms But Outcome Increasingly Grim" *Mars Daily*. <http://www.marsdaily.com/reports/Mars_Rovers_Brave_Severe_Dust_Storms_But_Outcome_Increasingly_Grim_999.html>

Moore, Henry J. (1985) "The Martian Dust Storm of Sol 1742" *Journal of Geophysical Research*. Vol. 90, Supplement, pp. D163-D174.

Parteli, Josef R. (2007) "Sand Dunes on Mars and Earth" PhD Thesis, University of Stuttgart.

Phillips, Tony. (1998) "Sand Dunes on Mars" *Science at NASA* October 29, 1998. <http://science.nasa.gov/current/event/ast29oct98_2.html>

Rizvi, Amjad Ali. (1983) "Planning Responses to Aeolian Hazards in Arid Regions" *Architecture and Planning* Vol. 1, pp. 59-74, Riyadh.

Sagan, Carl. and Kellogg, W. W. (1963) "The Terrestrial Planets" *Annual Review of Astronomy and Astrophysics*

Sheehan, William. (1996) "The Planet Mars: a History of Observation and Discovery" University of Arizona Press.

Sullivan, R., M. Golombek, R. Greeley, K. Herkenhoff, M. Kraft, J. Murphy, P. Smith, and G. Wilson,. (2000) "Results of the Imager for Mars Pathfinder Windsock Experiment" *Lunar and Planetary Science XXXI*

Sullivan, R. (2002) "Threshold-of-Motion Wind Friction Speeds at the Mars Pathfinder Landing Site." *Lunar and Planetary Science XXXIII*

Sullivan, R., D. Banfield, J. F. Bell III, W. Calvin, D. Fike, M. Golombek, R. Greeley, J. Grotzinger, K. Herkenhoff, D. Jerolmack, M. Malin, D. Ming, L. A. Soderblom, S. W. Squyres, S. Thompson, W. A. Watters, C. M. Weitz, and A. Yen. (2005) "Aeolian processes at the Mars Exploration Rover Meridiani Planum landing site" *Nature*. Vol 436 7 July 2005

Watson, J. M. (1997) "Desert Features" *USGS*. <http://pubs.usgs.gov/gip/deserts/features/>

Williams, KK (2006) "Are Martian Dunes Migrating? A Planet-Wide Search for Dune Movement" *Lunar and Planetary Science XXXVII* <http://www.lpi.usra.edu/meetings/lpsc2006/pdf/2322.pdf>

White, B. R. (1979) "Soil transport by winds on Mars". *Journal of Geophysical Research*, Vol. 84, pp. 643-651

Glossary of terms used in equations

$u(z)$	Wind velocity by height
z	Height above true surface
u_*	Wind shear velocity
κ	Von Kármán constant
z_0	Surface roughness
F_d	Drag force
β	Grain packing constant
σ	Particle density
d	Particle diameter
F_l	Lift force
p	Pressure
F_g	Force due to gravity
g	Planetary gravitational constant
ρ	Fluid density
τ_f	Shear stress
q	Sand mass flux

Appendix 1: Search for sand movement from HiRISE orbiting camera

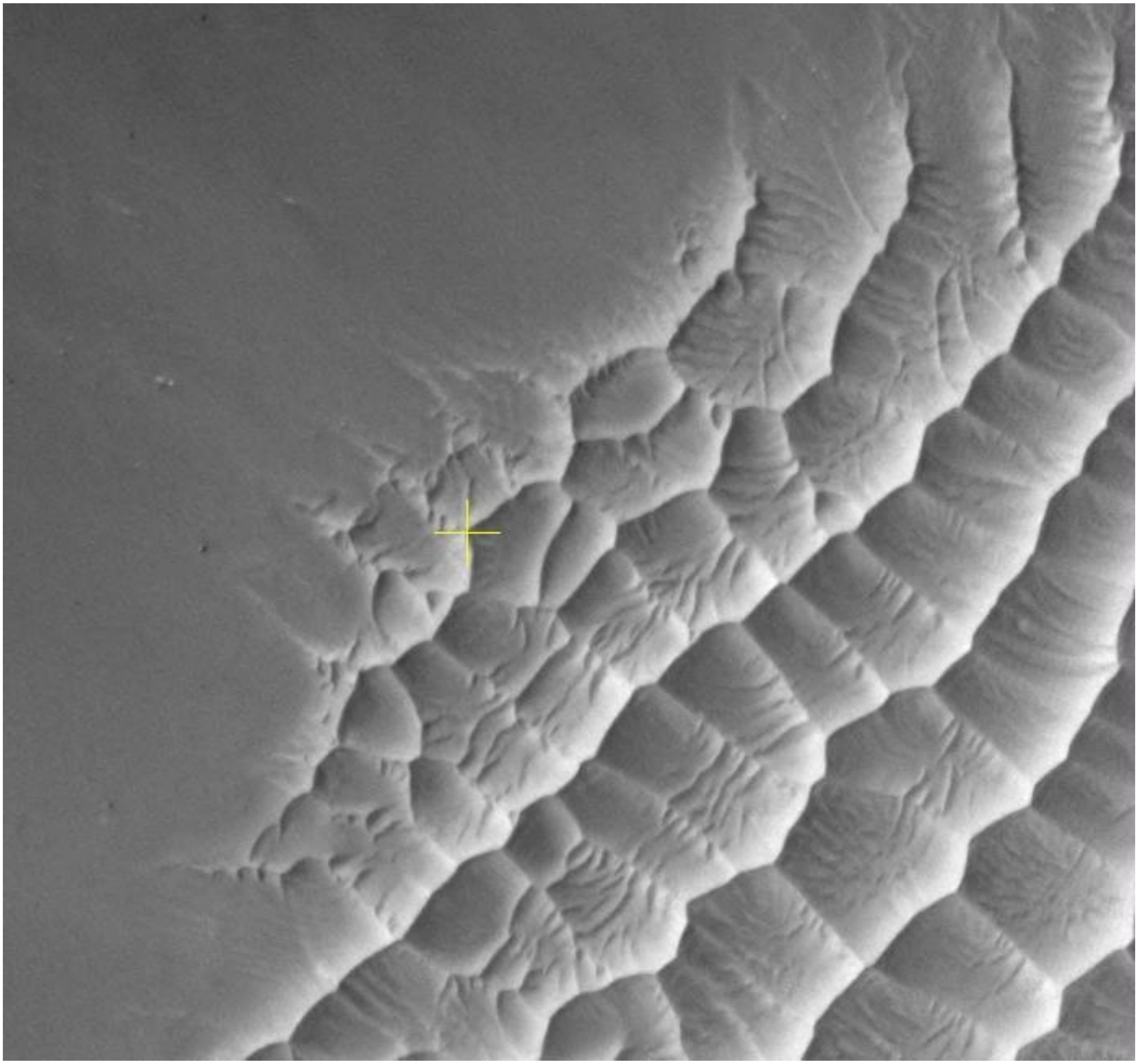

Image 1 (top): Taken 11-14-2006, resolution of 0.25m/pixel. A wider image for context is at right.

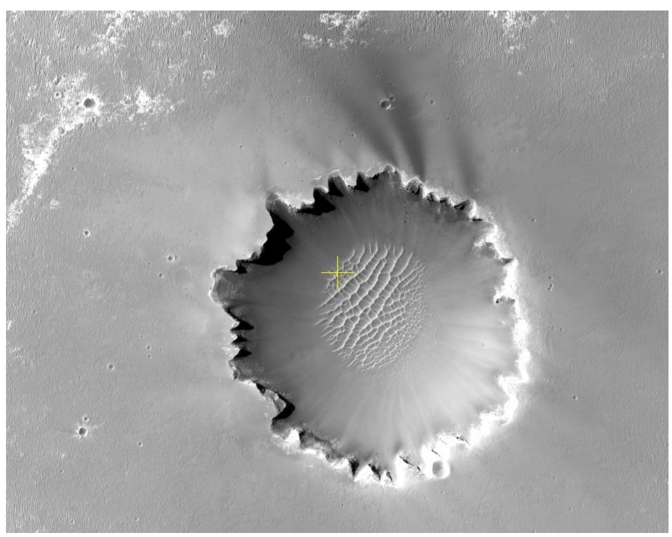

Image 2 (next page): Taken 01-11-2008, also at a resolution of 0.25 m/pixel. This image was taken at a different angle than the first, so a comparison with ImageJ was not possible. However, visual comparison showed no signs of deformation or movement, even in the small, intricate dunes near the edge.

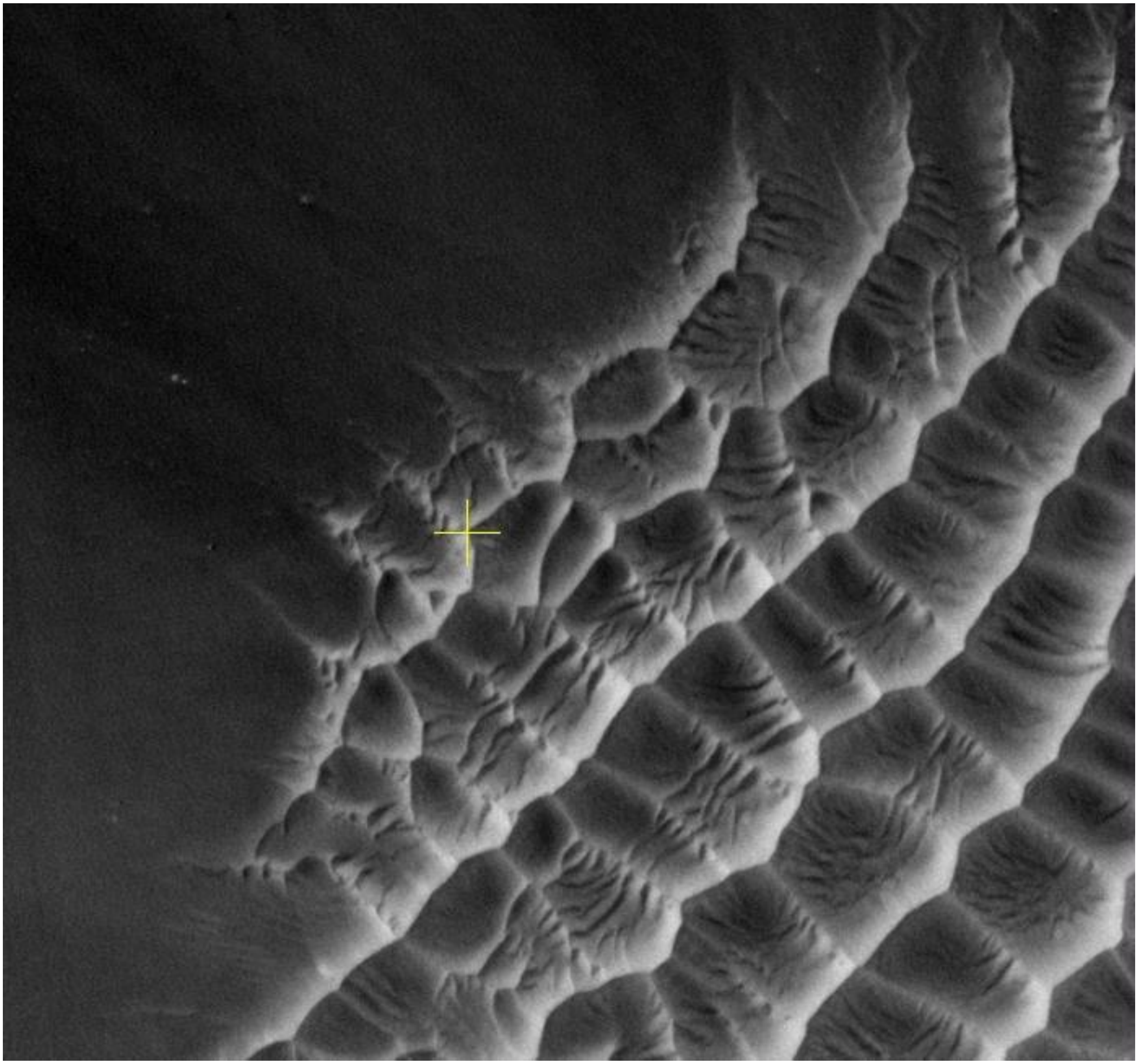

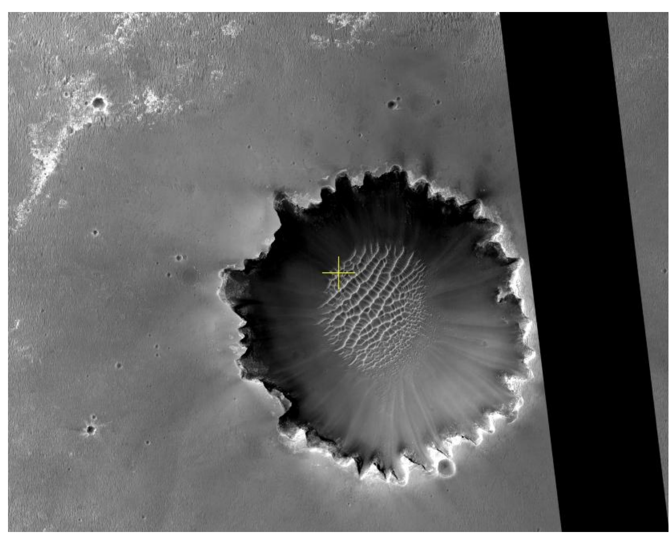

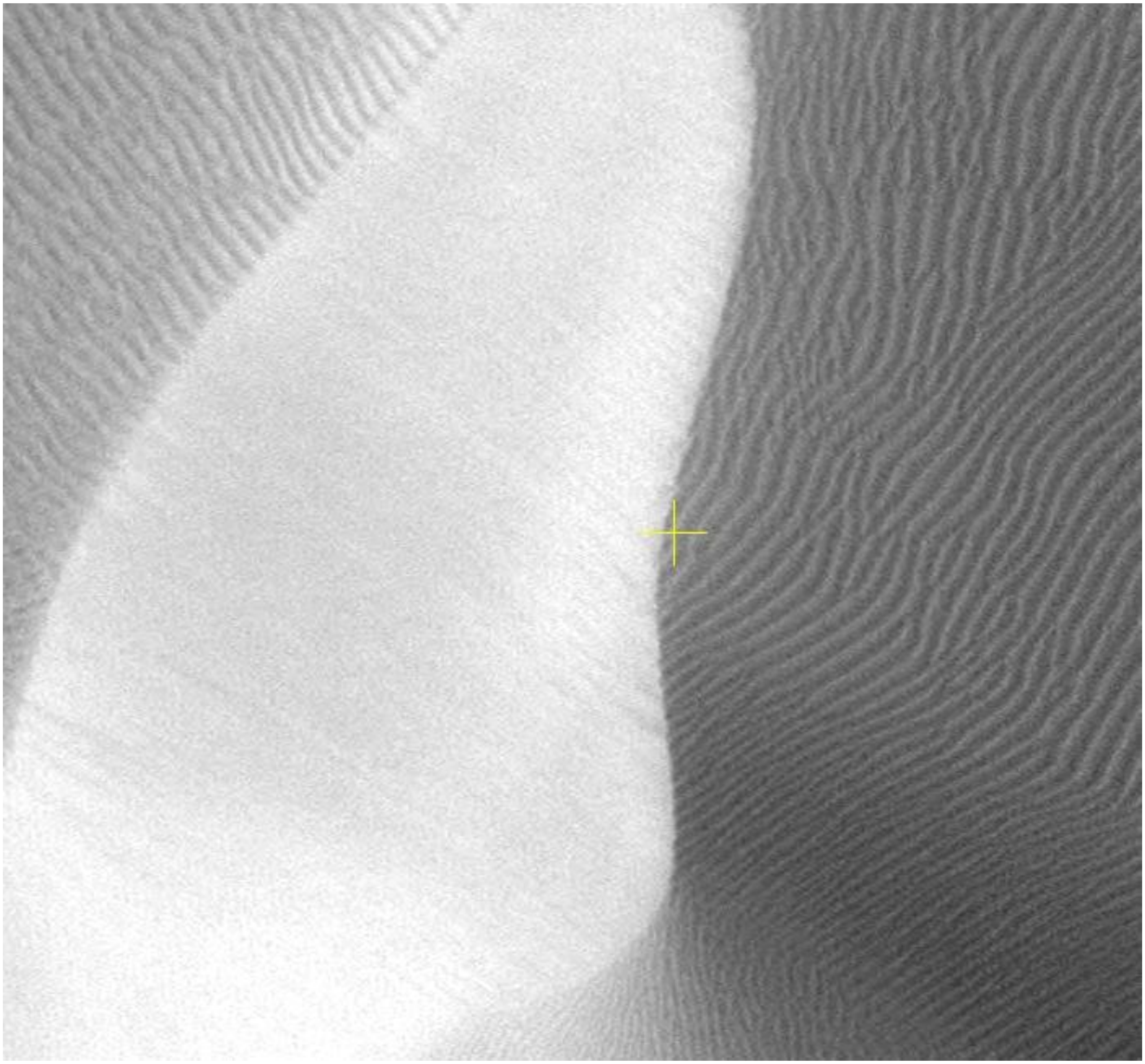

Image 3 (top): Image of a dune slip face in Rabe Crater, resolution of 0.25m/pixel. A wider image for context is at right.

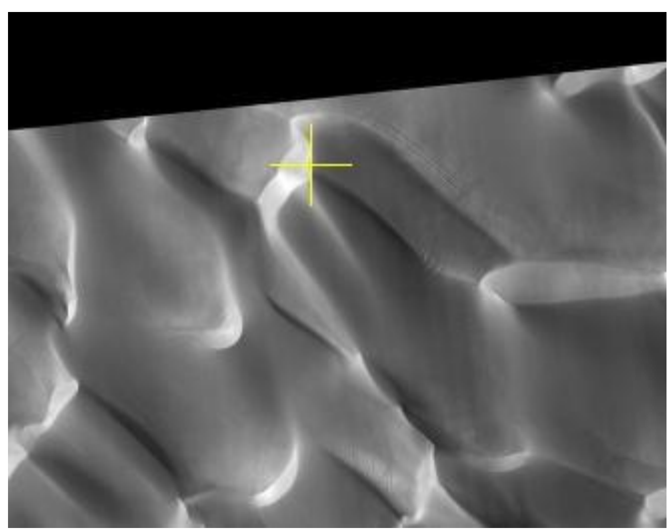

Image 4 (next page): The same slip face 39 days later, also at a resolution of 0.25 m/pixel. The same issue with image distortion is present, however, even the ripples near the dune crest show no change, not surprising with such a short timespan.

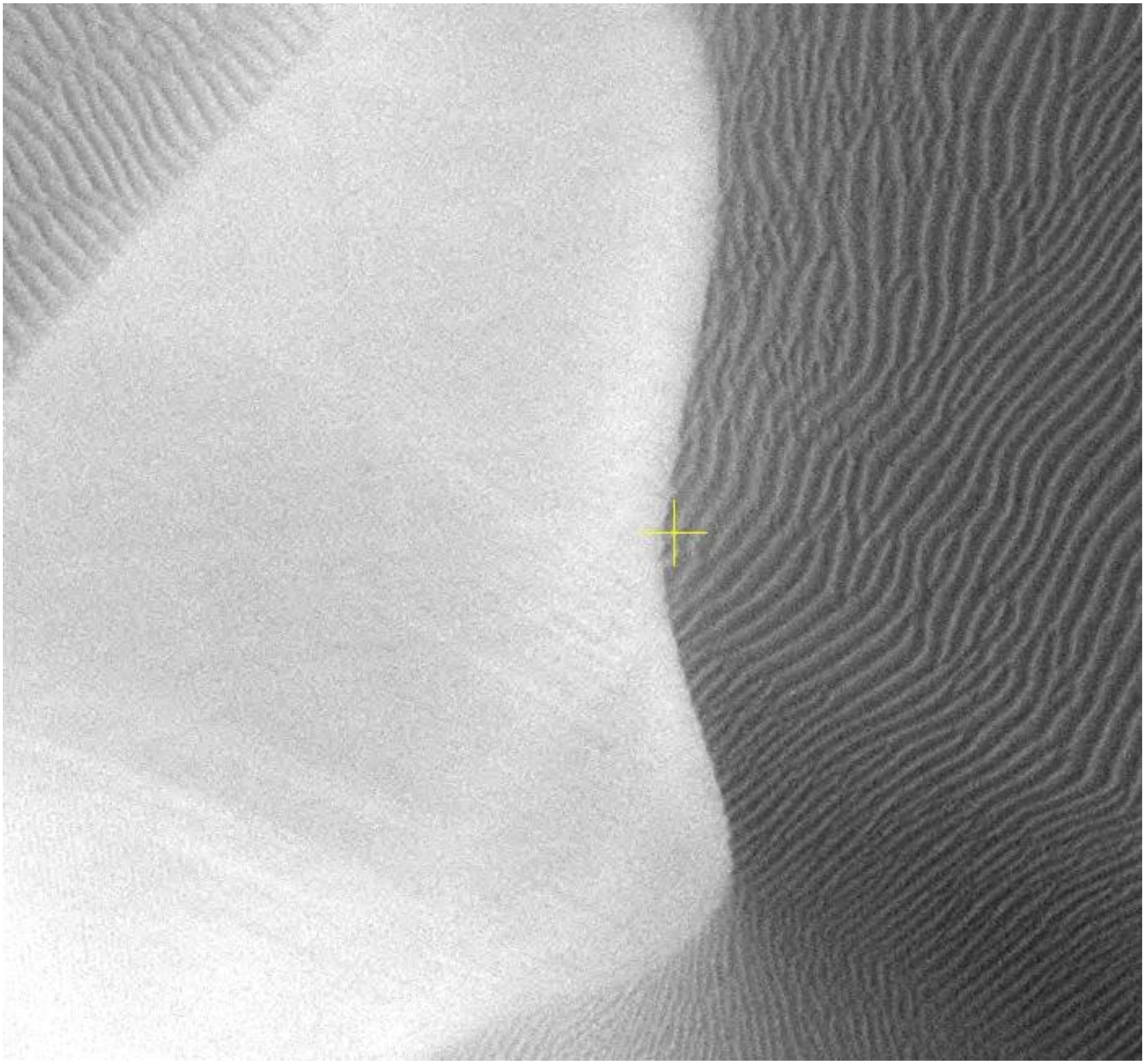

Appendix 2: Images used for determining grain size at Meridiani Planum

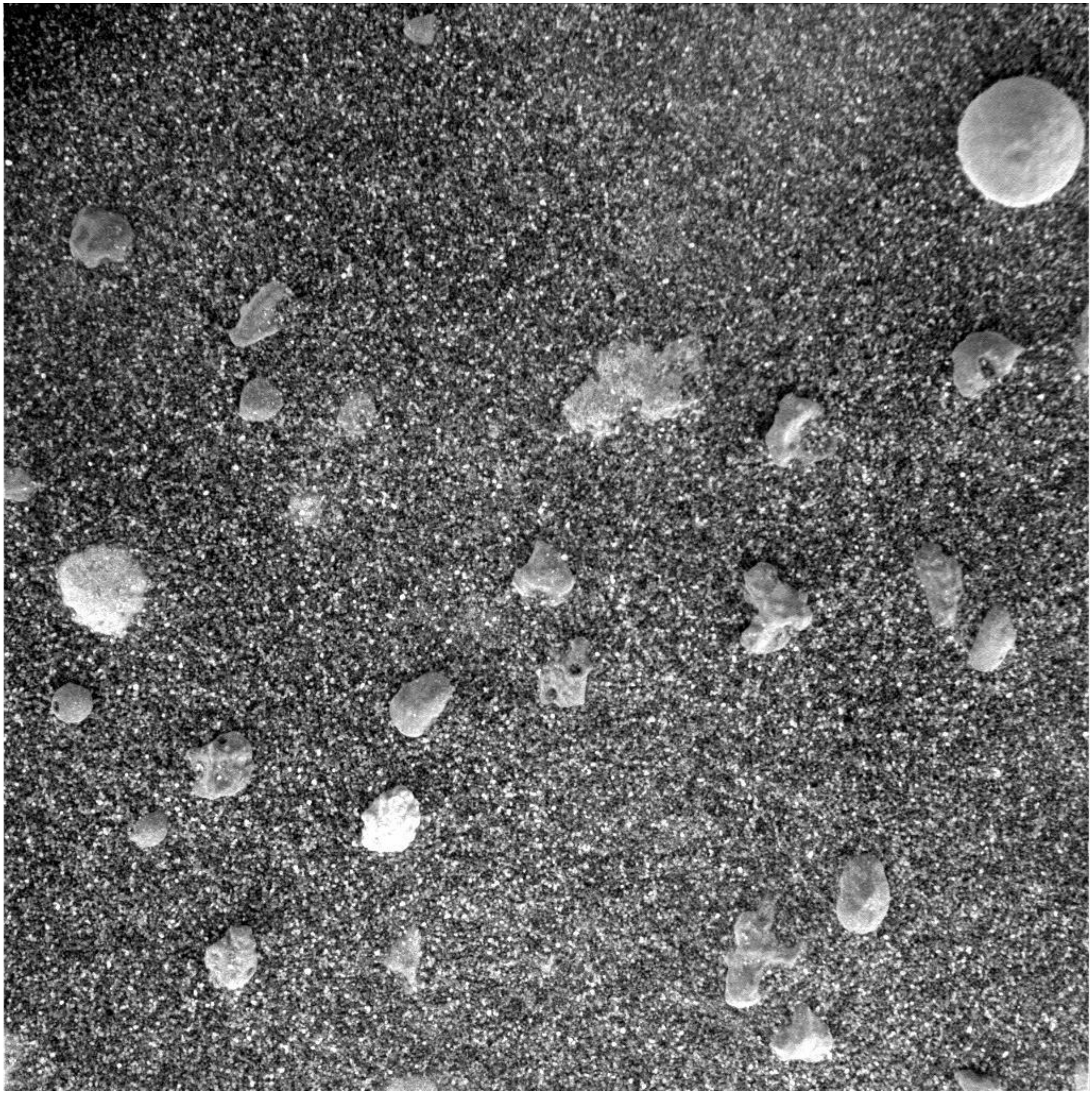

Sol 10: Sand on the floor of Eagle Crater

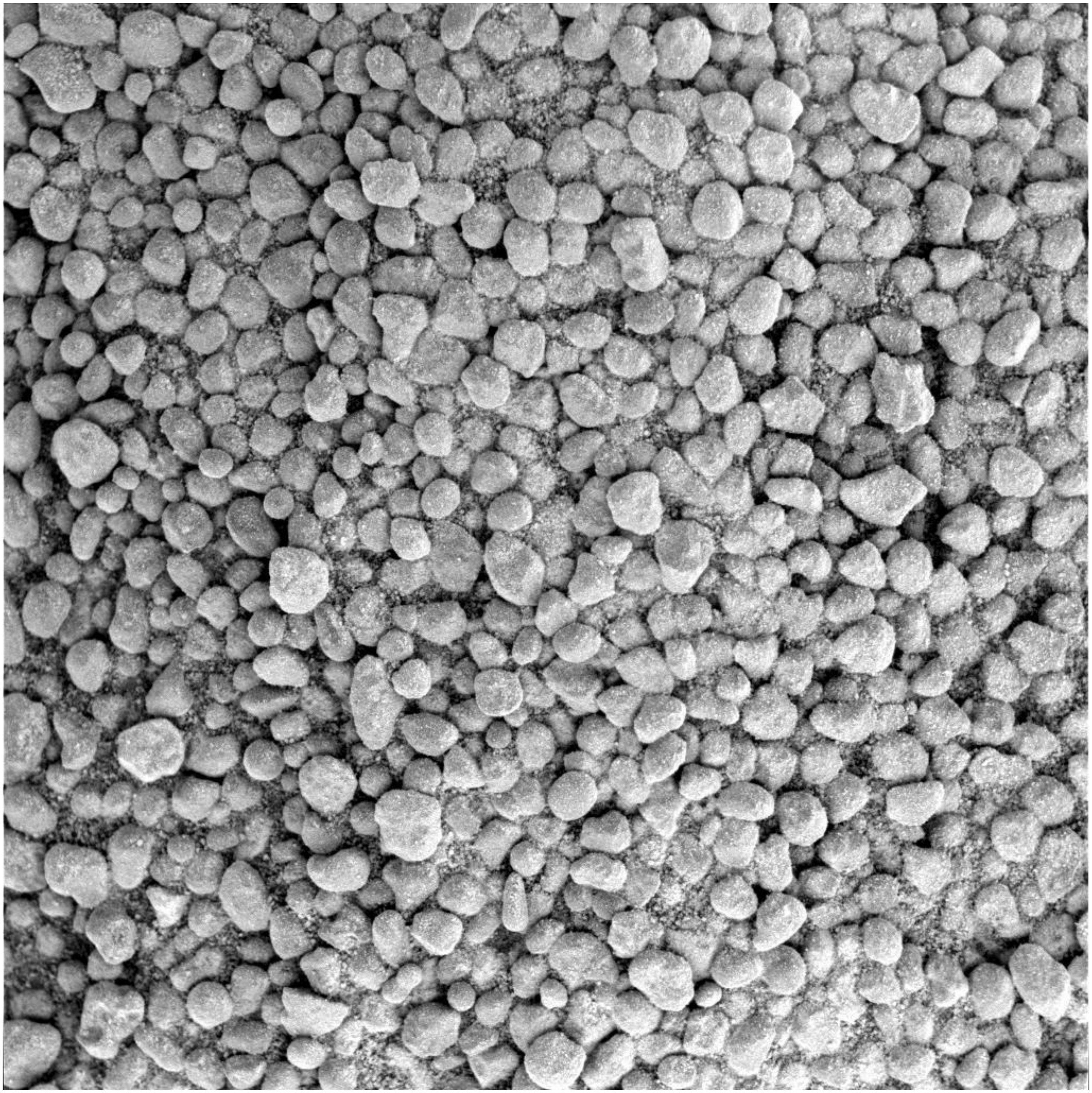

Sol 73: Ripple crest outside of Eagle Crater

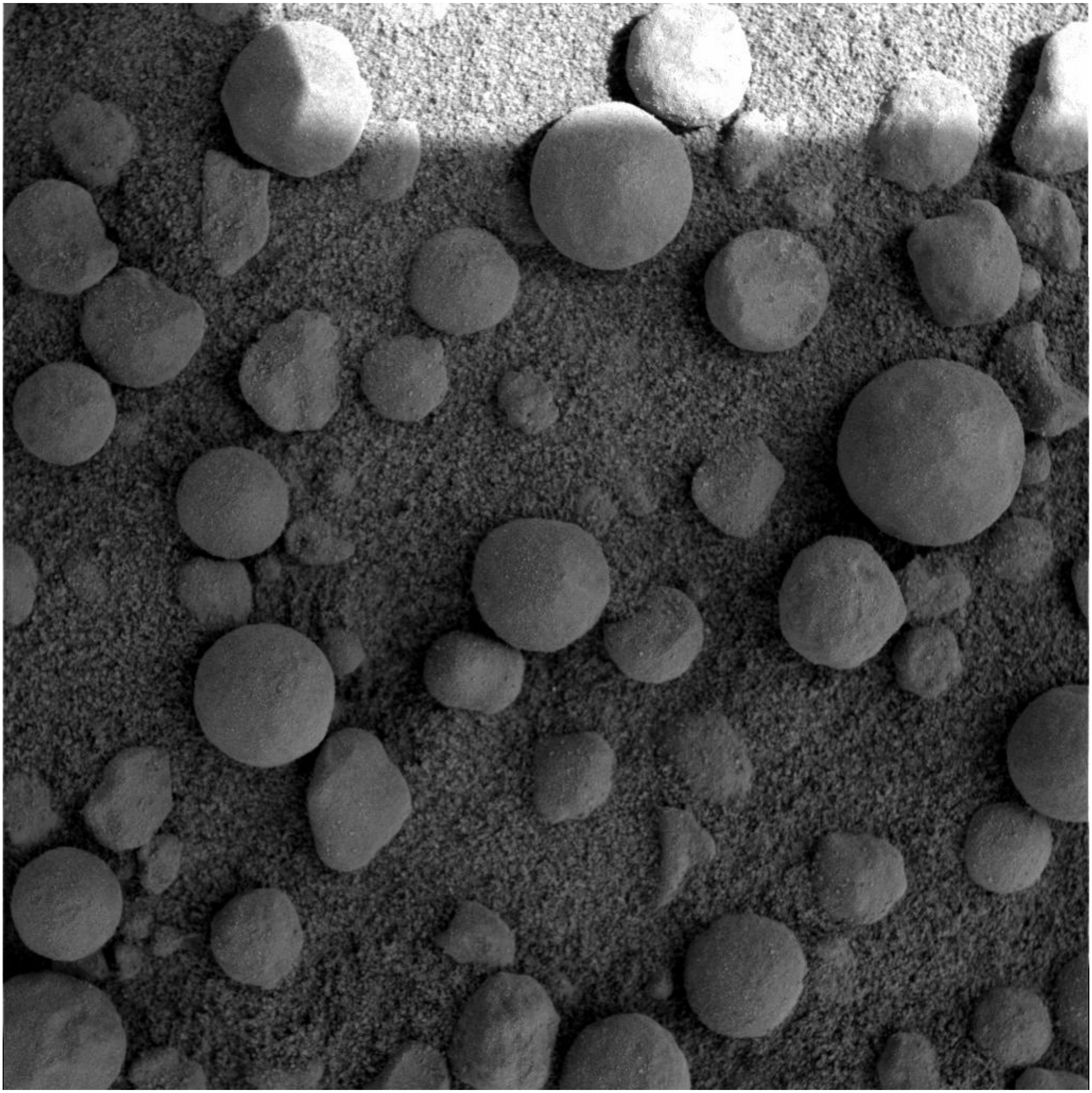

Sol 73: Ripple trough outside of Eagle Crater

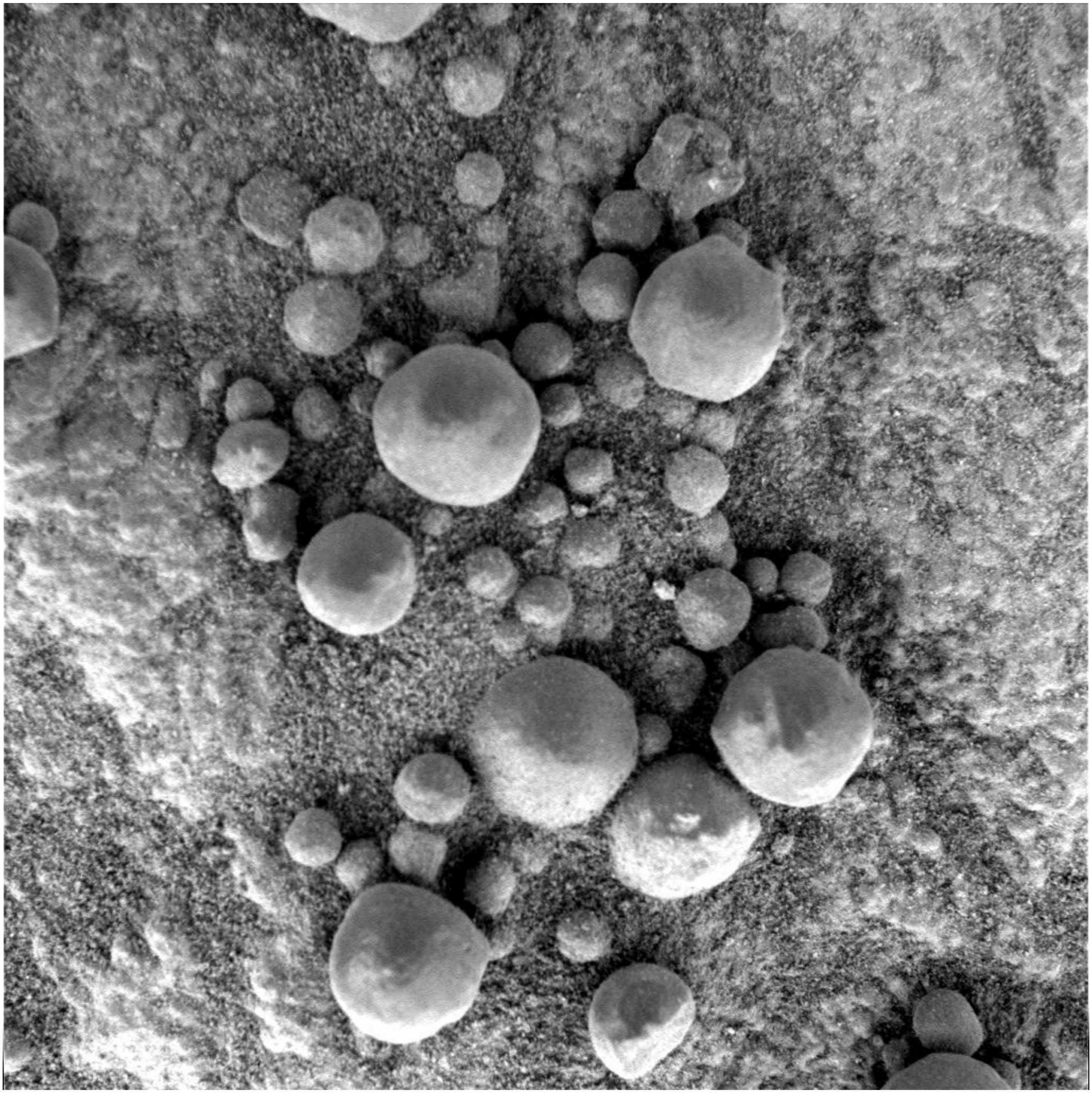

Sol 1216: Sand and pebbles on a rocky outcrop near Victoria Crater

Appendix 3: Full-resolution HAZCAM images from Sols 1232 and 1254

Sol 1232: Right HAZCAM image showing the view northeastward from the rim of Victoria Crater

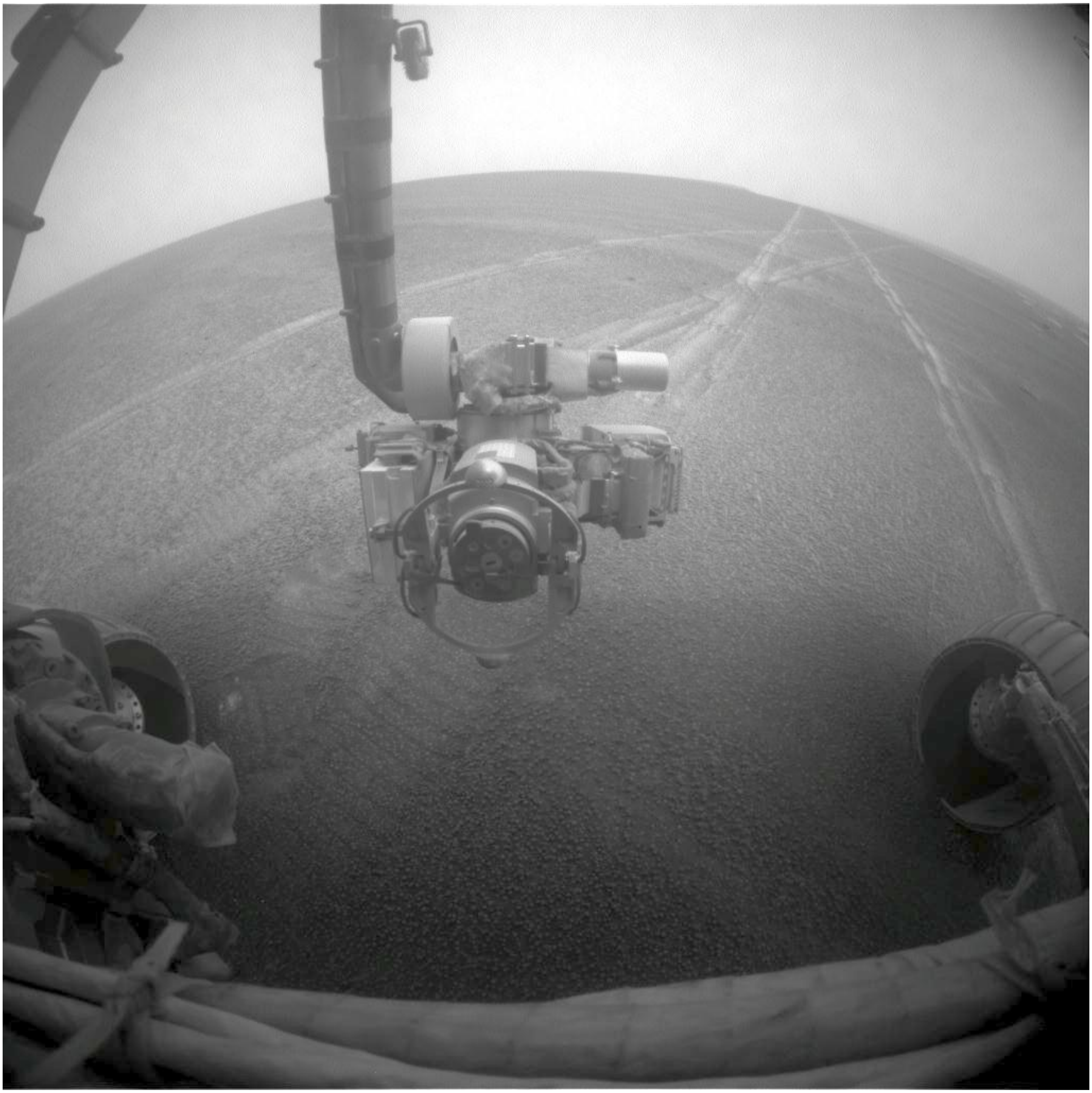

Sol 1254: The same scene, showing marked changes due to saltation. The object in the foreground is the rover's robotic arm, containing, among other things, the microscopic imager.